Three-Dimensional Numerical Manifold Method Simulations for Blocky Rock Analysis

By
Longfei Shentu
B.S., Civil Engineering (2010)
Nanyang Technological University

Submitted to the Department of Civil and Environmental Engineering in partial fulfillment of the requirements for the degree of

MASTER OF ENGINEERING IN CIVIL AND ENVIRONMENTAL ENGINEERING
AT THE
MASSACHUSSETS INSTITUTE OF TECHNOLOGY

JUNE 2011

Signature of author: _____
Department of Civil and Environmental Engineering
May 12, 2011

Certified by: _____
Jerome J. Connor
Professor of Civil and Environmental Engineering
Thesis Supervisor

Accepted by: _____
Heidi M. Nepf
Chair, Departmental Committee for Graduate Students

Three-Dimensional Numerical Manifold Method Simulations for Blocky Rock Analysis

By
Longfei Shentu
B.S., Civil Engineering (2010)
Nanyang Technological University

Submitted to the Department of Civil and Environmental Engineering
on May 12, 2011 in partial fulfillment of the requirements
for the degree of Master of Engineering in Civil and Environmental Engineering

Abstract:

After decades of development, people realize that there are wider and more various applications of numerical modeling and analysis. However, current feasible software tools cannot satisfy engineering and commercial goals. Therefore, a new generation of numerical modeling and analysis is imminent.

The implemented software tool is based on the 3-D version of the Numerical Manifold Method (NMM). Due to extremely complex situations caused by concave blocks, new and improved algorithms based on existing algorithms are implemented. Besides, in order to satisfy engineering requirements, support design based on block theory is also implemented.

Sufficient examples are elaborated in this report in order to illustrate the strength and feasibility of the proposed 3D-NMM software as if compares to current software tools. Moreover, various examples with further vertical and parallel development are needed in order to improve accuracy and efficiency.

Thesis Supervisor: Jerome Connor
Title: Professor of Civil and Environmental Engineering

ACKNOWLEDGEMENTS

First and foremost, I would like to express my sincere gratitude to my supervisor, Professor Connor for his invaluable guidance, profound vision, thoughtful suggestions, patience and encouragement in conducting this project. It has been a great privilege and honor to work with him. I wish for him and his family happiness and joy life.

Also, I want to express my gratitude for the support encouragement provided by all the members of M.Eng program, especially for Daniel Jimenez's great patience and help.

Finally, I must acknowledge the continual support and encouragement provided by my parents and friends, near and distant, for their help, understand and encouragement.

Table of Contents

LIST OF FIGURES

LIST OF TABLES

CHAPTER 1 INTRODUCTION

1.1 BACKGROUND

Year after year, highly prevalent and frequent geotechnical hazards have caused various kinds of catastrophic damage and fatalities. With raising of engineering consciousness regarding safety and economic concerns, an appropriate analysis tool to strengthen the understanding of failure mechanisms and reduce disastrous damage through efficient design is needed. However, there are few existing software tools suitable. Therefore, a recently proposed software tool which is targeting to build and analyze these geotechnical models based on the numerical manifold method (NMM) is implemented. It includes three main core parts, namely a 3-D block generation algorithm, contact algorithm, and support design. Most importantly, it has huge potential value in the rock engineering field.

Speaking of rock engineering, fracture is most often discussed and researched in this field. A fracture is any local separation or discontinuity plane in a geologic formation, such as a joint or a fault that divides the rock into two or more pieces. In the past decades, various numerical methods are proposed to characterize the mechanical behaviors of such discontinuities (fractures) in a computational model, either explicitly or implicitly.

For problems where the discontinuities can be implicitly modeled as a homogenization model, continuum-based numerical methods such as the finite element method (FEM), the finite difference method (FDM), and the boundary element method (BEM) can be adopted to be a representation.

On the other hand, there are also many problems where the explicit representation of discontinuities is desired. For FEM, the various interface element models, 'Goodman joint element' [Goodman et al., 1968], 'six-node fracture element' [Zienkiewicz et al.,

1970], 'thin-layer element' [Desai et al., 1984], 'joint element' based on the theory of plasticity [Ghaboussi et al., 1973], and 'interface element' in contact mechanics [Katona, 1983] have been implemented. However FEM requires the finite element mesh to conform cracks, therefore re-meshing is inevitable when fracture growth involved. In order to get away from the inconveniences caused by meshing and re-meshing processes, researchers have made some modifications to the conventional FEM based on the partition of unity (PU). Two representative examples are the extended finite element method (XFEM) [Moes et al., 1999 and Sukumar et al. 2003] and the generalized finite element mesh (GFEM) [Strouboulis et al., 2000]. In the XFEM, discontinuities and discontinuities in derivatives are directly represented by incorporating enrichment functions, while the GFEM increases the finite element approximation space with high-order terms or handbook functions of boundary value problems to tackle some typical problems with multiple reentrant corners, voids, and cracks.

Discontinuum-based numerical methods, such as the 'distinct element method' (DEM) [by Cundall, 1971] and the 'discontinuous deformation analysis' (DDA) [Shi, 1988], enable the analysis in discontinuous domains. However, they have a relatively inflexible description of block deformation and an insufficiently accurate description on stress field matters.

Numerical manifold method (NMM), proposed by Shi [1991], which combines all benefits of these methods, can be taken as a combination and transition of FEM and DDA through its important concept of manifold covers, namely mathematical and physical covers. The manifold cover is mathematically defined when the function is continuous and differentiable at each independent cover in the description domain. These overlapping mathematical covers create various manifold elements which generate the continuous and differentiable function description in whole domains, by intersecting with physical domains. Users are able to define geometrical shape, and

mathematical covers do not require conformation to the boundaries of their structures, thus remarkably reducing the workload of processing the meshes. An increase of underground construction and geotechnical work demands 3-D discontinuous deformation in reliable 3-D models. As a result, Cheng and Zhang [2008] derived one relatively basic theoretical formation of 3-D NMM without implementations.

The support design that protects structures from collapsing is of great importance in the field of underground projects, such as slope excavation and tunnel engineering. It is therefore important to develop methods to check the performance of the support design. So far, various models have been developed to simulate the system of rock mass, and several methods have been developed to check the performance of the system. Now, traditional methods, the Q-system and rock mass rating (RMR), are used in current underground projects. In Q-system rock mass classification [Lien and Lunde, 1974], six parameters including Deere's Rock Quality Designation (RQD), joint set number (Jn), joint roughness number (Jr), joint alteration or filling (Ja), joint water leakage or pressure (Jw) and Stress Reduction Factor (SRF), are used to characterize the rock mass quality. Three key aspects of the rock mass, block size (RQD/Jn), inter block shear strength (Jr/Ja), and active stress (Jw/SRF) are comprehensively considered by the Q-system. In RMR classification [Bieniawski , 1984], six parameters including uniaxial compressive strength of intact rock material, Rock Quality Designation (RQD), joint spacing, joint condition, ground water condition, joint orientation, are used to determine the rock mass quality. The six parameters in Q-system and RMR rock mass classification cover most of the mass classifications. However, it's extremely difficult to measure the values of these parameters from one specimen, and only geological experts can confirm the value of all the six parameters. It is therefore necessary to develop a method for the rock mass classification system with easy-to-obtain parameters.

Block theory [Shi, 1985] can be used for the performance checking of the support

design. In block theory, five parameters, cohesion, friction, dip and dip direction of joints, and rock density, are used to characterize the rock mass system. These parameters are easy to get and unique to one specimen. Thus, only the instability of the block is left for further consideration. Block theory is therefore a promising method for the performance checking of the support design.

1.2 OBJECTIVE AND SCOPE

The objective of this thesis is to simulate the response of 3-D engineering models with a NMM computer program which is suitable for analysis and support design of the underground structures, slopes, tunnels etc.

This thesis is focused on improving the 3-D block generation algorithm, modifying the Discontinuum version of 3-D NMM using an improved contact algorithm, and the support methodology based on block theory. Various examples of real applications are implemented in the thesis.

1.3 ORGANIZATION OF THE THESIS

This thesis contains 6 chapters. Chapter 1 provides a project background, objective and scope of the study. In chapter 2, a detailed literature review on numerical modeling for rock mass is presented. Chapter 3 gives a brief review on block theory which the proposed support design is based on. Chapter 4 illustrates the improvements and developments of the implemented 3-D NMM program. The idea of the proposed support design is presented in chapter 5. Finally, the application of implemented software tool is elaborated.

CHAPTER 2 LITERATURE REVIEW ON NUMERICAL MODELING FOR ROCK MASS

2.1 THE ROLE OF NUMERICAL SIMULATION

Numerical simulation based on computers or computational simulation has become a very crucial approach for solving complex practical problems in areas of engineering and science. Important characters of real physical problem can be translated into a discrete form of mathematical description. Thus, numerical simulation recreates and solves the problem through computer, and represents phenomena virtually according to the requirements of the analysts. Unlike the traditional theoretical method constructing layers of assumptions and approximations, with the help of the increasing computer power, this modern numerical simulation method attacks the original problems in all its detail without making too many assumptions,.

Numerical simulation is taken as an alternative for expensive, time-consuming or even dangerous experiments in laboratories or in-situ in scientific investigation. These modern numerical methods are often more useful than the traditional experimental methods when insightful and complete information is required, which cannot be directly measured or observed, or difficult to be acquired via the traditional methods.

Computer based numerical simulation also plays a valuable role in theory validation, offering insights to the results from experiments and assisting in the interpretation or even the discovery of new phenomena. Besides, it is important to connect the traditional models and theoretical predictions.

People prefer numerical methods in analysis of underground structures built in rock mass, since there are many limitations for theoretical or experimental approaches. However, the presence of discontinuities in the rock mass system, which usually appear in the form of faults, joints or bedding planes, is quite a challenge for

numerical simulation methods. Thus, to represent such discontinuities physically in the computer model has become one of the main tasks of numerical modeling. Moreover, there is still a long way to go for simulating the mechanical behaviors of rock mass, such as the discontinuous deformation, crack propagation fragmentation, and large-scale displacement.

In this chapter, a brief introduction of the numerical methods for rock mass will be given first. Comparison of the continuum method with the Discontinuum method is also discussed. Then basic concepts and theories of Numerical Manifold Method (NMM) will be given.

2.2 NUMERICAL MODELING FOR ROCK MECHANICS & ROCK ENGINEERING

2.2.1 The special nature of rock masses

The rock mass is largely Discontinuous, Inhomogeneous, Anisotropic and Not-Elastic (DIANE) [Harrison, 2000]. The discontinuities are mostly clustered in certain directions which are resulting from their geological modes and formation history.

In rock mechanics, one of the main tasks of numerical modeling is to be able to characterize those mechanical discontinuities in a computer based model either explicitly or implicitly in the so called 'material conceptualization'. Moreover, it is essentially necessary to incorporate the interaction between the rock mass and the engineering structure in the modeling procedure for design. Thus, it also needs to characterize the consequences of the construction process.

2.2.2 Difficulties in capturing the rock reality

The features described by DIANE can actually be translated into a computer based

model will depend on the physical processes involved and the modeling techniques adopted. Hence, subjective judgments will be contained in both the modeling and any subsequent rock engineering design [Jing, 2003]

Rock is a natural geological material and the physical or engineering characteristics have to be established rather than defined through a user define process. Hence, it becomes the reason for the general difficulty in modeling rock masses, by whatever numerical method. Besides, rock masses are under stress, strain, and continuously loaded by dynamic movements of the upper crust of the Earth, such as land uplifting or subsidence, tectonic movements, glaciations cycles, and earthquakes. Fluids in either liquid or gas phases, such as water, oil, air and natural gas, are trapped in a rock mass, since it is also a fractured porous medium which is under complex in-situ conditions of stress, strain, temperature, fluid pressures, extension.

The property of containing complex constituents and its long history of formation in a make rock mass makes it a difficult for mathematical representation via numerical modeling. So far, we can adequately represent capturing such fracturing, the complete DIANE nature of the rock mass, and the consequences of engineering the in a rock mass system via computational modeling yet.

However, the numerical model only needs to be adequate for the purpose, since it is almost impossible to be complete and perfect. Hence, the only challenge left is to know how to develop an adequate numerical model for our current engineering purposes. Due to this imperfect and useful property, rock mechanics modeling and rock engineering design are both a science and an art to some extent.

2.2.3 Numerical methods in rock mechanics

As the needs of designing and evaluating practical rock engineering structures increasing, researchers have developed rock mechanics simulation for decades with widely different purpose, and have developed a wide spectrum of numerical methods

to assist rock mechanics problems, which are categorized as:

(1) Continuum methods

(2) Discontinuum methods

(3) Hybrid continuum/Discontinuum models

For many problems, it can apply the mathematical assumption of an infinitesimal element to the whole domain of interest, which is termed continuous and with infinite degrees of freedom. At the field points, differential equations are inevitable for the description of the system behavior. In order to numerically solve these continuous problems, it is usually to subdivide the domain of interest into a finite number of sub-domains or elements, which is able to be easily approximated by simpler mathematical expressions with finite degrees of freedom. These sub-domains/elements essentially need to satisfy both the continuity condition at their interfaces with adjacent elements and the governing differential equations of the problem. In fact, a continuous system with infinite degrees of freedom can be approximated as the discretization of a continuum by a discrete system with finite degrees of freedom [Jing, 2003]. Hence, numerical methods based on the above-mentioned system are termed as continuum-based numerical methods.

From a geological structure viewpoint, rock blocks can be considered as a system of blocks cut by planes in space [Chen et al., 2002]. These geological planes which are commonly termed as discontinuities could be faults, joints, or cracks. The most important discontinuous planes for rock systems are the major structural planes, such as faults, large crack, and large joints. The geometrical distribution and physical properties of discontinuities considerably act the mechanical behavior of a jointed rock system [Chappell, 1979] [Hoek and Bray, 1977]. However, the assumption of displacement continuity across elements is a fundamental deficiency of using the conventional continuous-based methods. Even to use the likewise interface element

alone without the displacement continuity assumption, it is not always adequate to solve the problems reasonably. When the large deformations and displacements of the rock masses occur, the continuum methods can not satisfy the circumstances.

Hence, discontinuum methods are developed to solve the problems. These approaches should only maintain the continuity of the elements within an element. Besides, its displacement function should be considered to be discontinuous across element boundaries. Several computational rock mechanics methods focus on the study of these rocks systems, such as distinct element method (DEM) [Cundall, 1971], Discrete Fracture Network method [Long et al., 1982], block theory [Goodman and Shi, 1985], and discontinuous deformation analysis (DDA) [Shi, 1988].

However, it is often the case that individual discrete blocks are also able to fracture, which is in fact a transition process of from continuous to discontinuous. The combined continuum-based and discontinuum-based numerical methods are able to represent these problems well, such as the numerical manifold method (NMM) [Shi, 1991] and the combined finite-discrete element method [Munjiza, 2004].

2.2.4 Numerical manifold method (NMM)

Numerical Manifold Method (NMM) is firstly proposed, by Shi [Shi, 1991] at Berkeley, as an extension of DDA. It is a relatively flexible numerical method which combines and contains finite element method (FEM) and discontinuous systems considered in DDA in a unified form. This method is applicable to a much wider range of situations, since it combines the advantages of both DDA and FEM together.

NMM uses so called continuous and discontinuous cover functions to solve problems in their continuous and discontinuous domains. Moreover, it is possible to reduce this method into the classical finite element method (FEM) and DDA. However, it can be used for more general circumstances that are found in various practical geotechnical problems than FEM and DDA.

Almost all current NMM cover functions are adopted directly from finite element shape functions, since the development of various techniques in FEM is relatively mature. Instead of using higher order cover functions, it is preferred to adopt simple cover functions for NMM to avoid complicated formulation and simplify the computational process.

The researchers [Cheng and Zhang, 2002] have however shown that more accurate results for simple covers can be obtained by using the more advanced 2-D Wilson non-conforming elements to NMM. Hence, for a proper NMM analysis, it is hence also important to make a choice of cover function, particularly when the sizes of blocks are remarkably large.

Due to their natures, practical geotechnical problems are generally in three dimensions, including the geometry of the construction works, the discontinuities, and the properties of the various rock materials. So far, 3-D-DEM has been developed by Cundall [Cundall, 1985] in a DEM code 3DEC while there are some simple implementations of 3-D-DDA by Wang [Wang, 1996], Jiao [Jiao, 1998], Jiang [Jiang, 2000], and the researchers [Cheng and Zhang, 2002]. However, the majority of current NMMs are limited to two-dimensional analysis. Although it is very important for engineering problems, there is few research works in the 3-D development. The major challenging difficulties for three-dimensional NMM are:

(1) Definition of cover functions;

(2) 3-D contact detection;

(3) 3-D contact stress-strain relation.

2.3 BASIC CONCEPTS AND THEORIES OF NMM

2.3.1 NMM components

As shown below in Fig. 2-1, three fundamental concepts in the NMM, the mathematical cover (MC), the physical cover (PC), and the cover-based manifold element (CE), are presented.

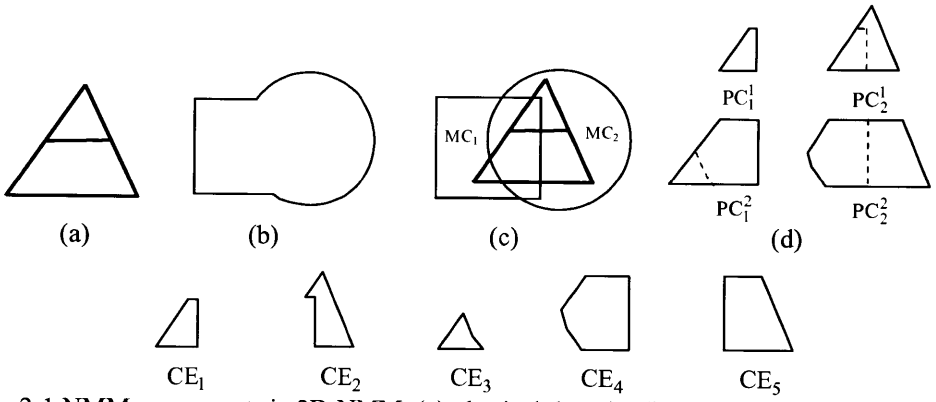

Fig. 2-1 NMM components in 2D-NMM: (a) physical domain; (b) mathematical domain; (c) mathematical covers; (d) physical covers; (e) cover-based manifold elements

Problem domain refers to the domain where physical problem is defined. Fig. 2-1a shows the 'physical domain', where the external geometries on which boundary conditions are prescribed, all physical features and problem domain in which the physical problem are defined. Fig. 2-1b shows a domain which is independent but completely cover the physical domain is called the 'mathematical domain'.

A finite number of small elements, called mathematical covers, denoted as MCI, consist of the mathematical domain. Moreover, the mathematical covers, which are user-defined, can have an arbitrary shape and overlap each other partially or completely. Thus, they are defined completely independent from the physical domain. However, their union must be large enough to cover the entire whole physical domain. In Fig. 2-1c, MC1 and MC2 are two mathematical covers of the physical domain.

The physical covers are defined as the intersection of mathematical covers and the physical domain. A mathematical cover MCI will be partitioned into several physical covers, denoted as $PC_I^j (j = 1 \sim m_I)$, when it is completely cut by the physical features. As shown in Fig. 2-1c, MC1 is completely cut into three isolated parts by the physical features, and two of them are within the problem domain. Hence, as shown in Fig. 2-1d, two physical covers, PC_1^1 and PC_1^2, two physical covers are formed.

The common region shared by several physical covers defines a cover-based manifold element. As shown in Fig. 2-1e, five cover-based manifold elements are formed from the four physical covers in Fig. 1d.

In Fig. 2-2a, it illustrates the three basic components of the 3D-NMM, the mathematical cover (MC), the physical cover (PC), and the cover-based manifold element (CE). There is one sphere mathematical cover and one hexahedron mathematical cover in total, denoted as MC1 and MC2. The pyramid defines the physical domain. In Fig. 2-2b, two physical covers PC_1^1 and PC_2^1 are generated. As shown in Fig. 2-2c, three cover-based manifold elements, CE1, CE2, and CE3, are formed from the two physical covers.

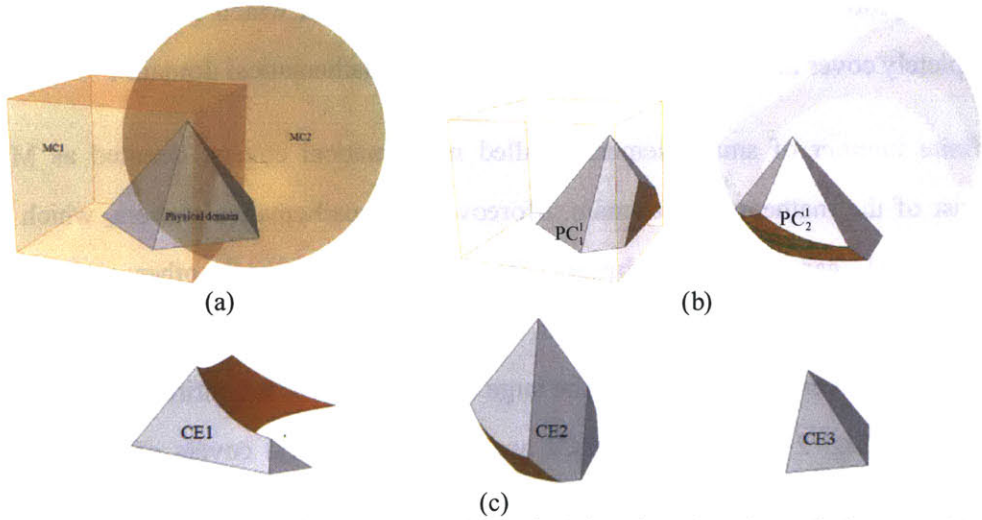

Fig. 2-2 NMM components in 3D-NMM: (a) physical domain and mathematical covers; (b) physical covers; (c) cover-based manifold elements

2.3.2 *NMM approximations*

The weight function $\varphi_I(\mathbf{x})$ on each mathematical cover MCI, must satisfy

$$\begin{aligned} &\varphi_I(\mathbf{x}) \in C^0(\mathrm{MC}_I) \\ &\varphi_I(\mathbf{x}) = 0,\ \mathbf{x} \notin \mathrm{MC}_I \end{aligned} \tag{2-1a}$$

$$\sum_{\substack{K \\ \text{if } \mathbf{x} \in \mathrm{MC}_K}} \varphi_K(\mathbf{x}) = 1 \tag{2-1b}$$

The weight function $\varphi_I(\mathbf{x})$ has non-zero value only on its corresponding mathematical cover MC_I, but zero elsewhere, as shown in Eq. (2-1a). It also indicates that it is continuous over the mathematical cover MC_I. Moreover, Eq. (1b) is called the partition of unity (PU) for the continuity of approximation.

On PC_I^j, physical cover, cover function denoted as $\mathbf{u}_I^j(\mathbf{x})$ is defined. Weight functions defined on each MC transfer to PC as

$$\varphi_I^j(\mathbf{x}) = \delta_I^j \cdot \varphi_I(\mathbf{x}) \tag{2-2}$$

where δ_I^j is a modify parameter, with the value of 1 within the physical cover PC_I^j and zero elsewhere. For physical cover PC_I^j, it has two indices, *I* and *j*. Instead of *I* and *j*, a single index *I* is used in order to simplify the implementation, shown as:

$$i(I, j) = \sum_{l=1}^{I-1} m_l + j \tag{2-3}$$

Then, PC_I^j, $\mathbf{u}_I^j(\mathbf{x})$ and $\varphi_I^j(\mathbf{x})$ are simplified as PC_i, $\mathbf{u}_i(\mathbf{x})$ and $\varphi_i(\mathbf{x})$, respectively. Now, the combination of the weight functions $\varphi_i(\mathbf{x})$ and cover functions $\mathbf{u}_i(\mathbf{x})$ indicates a global approximation over each cover-based manifold element as

$$\mathbf{u}^h(\mathbf{x}) = \sum_{\substack{i \\ \text{if } \mathrm{CE} \subset P_i}} \varphi_i(\mathbf{x}) \cdot \mathbf{u}_i(\mathbf{x}) \tag{2-4}$$

Various high-order terms and special functions can be substituted into the cover

functions to obtain a more accurate approximation, since the PU property of the weight functions.

2.3.3 Imposition of essential boundary condition

As stated above, the mathematical covers, MC are constructed completely independent of the boundaries of physical problems. Unlike FEM, it is not possible to accomplish the essential boundary condition by directly enforcing the degrees of freedom, in the NMM. However, the Lagrange multiplier method, the penalty method and the augmented Lagrange multiplier method in the weak form of governing equations [Ma et al., 2009] can help obtain the essential boundary condition.

2.3.4 Contact problems in the NMM

The main purpose of the NMM is to solve the discontinuous problems, even with rigid movements or large distortion. Each mathematical cover (MC) can form several independent physical covers (PC) with individual cover functions when it is intersected discontinuities. Hence, the adjacent cover-based manifold elements, which are formed by these physical covers (PC), are independent on each other in the NMM.

In fact, the cover-based manifold elements on the two sides of the discontinuities are not completely independent, but with some relations. For instance, when a problem domain of physical problem is containing a strong discontinuity, the displacement field across the crack surface is discontinuous. On the other hand, the upper side and the lower side of a crack surface cannot penetrate through each other in geometry even under a complex stress state. The kind of the problems with discrete bodies is another example. The displacement field is discontinuous. However, one body cannot penetrate through another body. These constraints are regarded as non-penetration or unilateral condition, and attributed to the contact problems in physics.

Hence, NMM adopts an incremental approach for generality of nonlinear and irreversible frictional contact problems. At the beginning of the current time step, the contact state is known. On the other hand, after a time interval of step time, the

contact state at the end of the current step is to be solved. Moreover, it is essentially necessary to choose a time incremental for each time step small enough in order to make displacements of all the points less than a predefined maximum displacement limit ρ. Through the open-close iteration, no penetration and no tension of the two sides of discontinuous entities, two contact constraints will be fulfilled. For more details on contact detection and modeling in the 2D-NMM can refer to Shi [Shi, 1991].

CHAPTER 3 LITERATURE REVIEW ON BLOC THEORY

Excavations are crucial to both mining and various civil engineering projects. Reinforcement becomes an essential part of the projects, for both economic and safety concerns. However, it lacks a formal terminology and the rational design procedures for the reinforcement of jointed rock.

Due to many parameters involved, there is no rigorous engineering design approaches for jointed rock so far. Hence, design approaches based on basic description of rock mass are particularly popular. Moreover, the precedent rules [Lang, 1991] and mass classification methods [Barton et al., 1974] are the ones following this. However, the nature and disposition of the discontinuities adjacent to the excavation define the surface of rock mass and influence its stability. Reliable support designs are associated with addressing these instabilities. It indicates that good support design can only base on the examination of the assemblage of surface blocks. However, few methods are proposed based on block theory [Goodman and Shi, 1985], except the rock reinforcement system [Windsor, 1997].

3.1 REINFORCEMENT TERMINOLOGY

Although support design has advanced for decades, the current jargon is still complicated and confusing. In order to develop it into a formal engineering discipline, a formal terminology is extremely crucial. Moreover, it may help simplify the problems. Hence, the most common used terminologies are summarized here.

3.1.1 Rock improvement

It is a collective term including all methods aiming to improve the mechanical properties and desirable attributes of a rock mass. Rock improvement includes all

methods to increase the strength and reduce the deformability of the rock mass, such as rock support, rock reinforcement, etc. It is a subset of ground improvement which is generally accepted in civil engineering practice.

3.1.2 Rock support and rock reinforcement

Support is considered as the application of a force applying at the face of excavation, including all devices and techniques. For instance, timber, concrete sets, steel, etc. On the other hand reinforcement is an improvement of the overall rock mass properties, such as anchors, bolts, etc.

3.1.3 Pre-reinforcement and post-reinforcement

Pre-reinforcement is the reinforcement prior to the activity of excavation. While, post-reinforcement is the reinforcement at a proper time after the activity of excavation.

3.1.4 Pre-tensioned and post-tensioned reinforcement

Pre-tensioned reinforcement is to apply an initial tension to the reinforcement system during the installation. On the other hand, post-tensioned reinforcement is to tension or re-tension the system subsequent to initial installation.

3.1.5 Permanent reinforcement and temporary reinforcement

Referred to the requirement of service life, permanent reinforcement and temporary reinforcement refer to an extended service life and a limited service life, respectively.

3.1.6 Primary, secondary and tertiary reinforcement

Primary reinforcement refers to the reinforcement of maintaining overall stability. Moreover, secondary reinforcement refers to the reinforcement of securing medium to

large blocks or zones of rock between the primary reinforcement. Finally, tertiary reinforcement refers to the reinforcement used in conjunction with surface restraint to prevent surface loosening and degradation.

3.1.7 Types of reinforcement devices and techniques

They are generally categorized as:

(1) Rock bolts and rock bolting (less than 3 meters in length)

(2) Cable bolts and cable bolting (from 3 meters to 15 meters in length)

(3) Ground anchors and ground anchoring (longer than 10 meters in length)

The tensile capacity of these reinforcements is related to the reinforcement element length, termed as 'length-capacity relation'. Moreover, the length-capacity relation and the notion of primary, second and tertiary reinforcement are related.

3.1.8 Types of reinforcement scheme

The reinforcement scheme is referred as an arrangement of primary, secondary and tertiary reinforcement systems associated with various dimensional and spatial configurations. The spatial configurations could be pattern reinforcement, spot reinforcement and combination reinforcement. Furthermore, there are two fundamental reinforcement patterns, rectangular array and oblique array.

3.2 REINFORCEMENT SYSTEMS

3.2.1 The load transfer concept for reinforcement systems

This concept is consisting of three basic mechanisms:

(1) Rock load and movement transfer from the unstable zone to the reinforcing

element.

(2) Load transfer from the unstable region to a stable interior region via the element.

(3) Transfer from the element to the stable rock mass.

These are the critical steps in design of reinforcement system.

3.2.2 The reinforcement system concept

The reinforcement system is consisting of four principal components:

(1) The rock

(2) The element

(3) The internal fixture and

(4) The external fixture

Each component is involved in the process of load transfer. The concept is crucial, since the overall behavior of the reinforcement system is indicated by the component interactions of the system. Hence, it is important for understanding the mechanics of reinforcement behavior, the design if tests for laboratory and in-situ mechanical properties of reinforcement.

3.2.3 *The fundamental classes of reinforcement system*

Three most commonly used types are shown as:

(1) Continuously Mechanically Coupled (CMC)

(2) Continuously Frictionally Coupled (CFC)

(3) Discretely Mechanically or Frictionally Coupled (DMFC)

This classification is valid for all commercial reinforcement devices, since it is based on the extent and degree the device coupled to the rock.

3.2.4 Reinforcement system response

This term refers to the mechanical behavior of a reinforcement system in response to an excitation or disturbance in the rock mass. The response depends on various parameters, such as the arrangement of the reinforcement and force displacement field set up by the excitation. Moreover, the most common response is the combination of axial, shear, tensional or flexural.

Also, the behavior of a reinforcement system is determined by the principal components of the system and their interactions. It therefore indicates that the response of one or more principal components or the interaction between two components may determine the overall response of the system. Hence, it is necessary to optimize the individual component in order to optimize the overall response of the system.

3.2.5 Reinforcement system capacity

Two crucial terms are declared below, System Force Capacity and System Displacement Capacity. System Force Capacity (F_c) is the maximum force the system can afford, and associated with a displacement. On the other hand, System Displacement Capacity (δ_c) is the maximum displacement the system can afford, and associated with a force.

3.2.6 Types of reinforcement system response

Obviously, there exist various reinforcement system responses. However, they can be reduced to limited types according to the mechanical and physical properties of the principal components. There are clearly differences which will influence the

suitability of a given system to a given set of in-situ requirements between different types of responses.

3.2.7 Reinforcement system utilization and mobilization factors

The response may result in a new state of equilibrium or failure of the system. When it is the state of equilibrium, the force and displacement capacity, and principal components are partially utilized. On the other hand, some components are fully utilized in terms of force and displacement, and the others are only partially utilized at failure.

Utilization equals to mobilization factor expressed as a percentage. Assuming the service load F_s and service displacement δ_s, mobilization factors are F_s/F_c and δ_s/δ_c, since they are related to the system capacity.

3.2.8 Reinforcement scheme response

A reinforcement scheme is a global system comprising multiple subsystems, including system capacity system response, etc. Its behavior depends on both natural components and artificial components, and their interaction.

However, it is more complicated and difficult to determine the behavior of reinforcement scheme than the behavior of reinforcement system. It is possible to estimate the reinforcement scheme by applying numerical and analytical procedures to rock mass mechanisms, in some cases. Unfortunately, in most cases, a formal solution is not possible. Hence, an appropriate reinforcement scheme is best based on numerical and analytical procedures to the system.

3.3 KEY BLOCK METHOD

Block theory, firstly proposed by Goodman and Shi, is a 3D geometrical method for

rigorous inventory and analysis of rock blocks. It is consisting of mode analysis, removability analysis, and stability analysis. A list of removable blocks which can move into the free space is given by the removability analysis. However, the mode of failure also determines whether it will move or not, which is determined by mode analysis. Then stability analysis is conducted on 'keyblocks' which will fail without external support. It is therefore only necessary to check the stability of keyblocks instead of whole rock mass, since the whole rock mass is stable when all the keyblocks are stable. It indicates the beauty of simplicity of block theory, which narrows the range of checking.

So far, there are still limitations to the mode and stability analysis. At the very beginning, Goodman and Shi only took pure sliding into consideration. Recently, there are extensions including special rotational modes of a special block shape, i.e. corner rotation and edge rotation of tetrahedral blocks, by Mauldon and Goodman [Mualdon and Goodman, 1996], and Tonon [Tonon.1998]. This is a new start that is providing a procedure to handle general modes of simultaneous sliding and rotation.

CHAPTER 4 IMPROVMENTS AND DEVELOPMENTS OF THE PROPOSED 3-D NMM PROGRAM

4.1 GEOMETRIC CONFIGURATION OF 3-D MATHEMATICAL COVER

4.1.1 Geometric patterns

The most fundamental concept is Geometric Pattern (GP), GP is a type of theme of the recurring objects, sometimes considered as elements of a set, to generate space or parts of an object [Nooshin *et al.*, 1997]. In the implementation of 3-D NMM, the first step is to select a basic GP to fill the entire 3-D space, which is essentially same as in the implementation of 2-D NMM. In most cases, GP geometry is based on platonic solids (see Fig. 4-1). The first three basic polyhedrons are commonly used, while other polyhedrons as shown are still seldom used to form up the space in other fields. Hence, the NMM is a possible platform where the applications of different platonic solids can be extended to. However, for computational efficiency and convenience, simple and regular geometric patterns are recommended. For the reason of with high identity and uniformity, the equilateral triangle and rectangle are the excellent choices for the 2-D NMM. However, the regular tetrahedron is not sufficient to fill up the entire 3-D space. Consequently, a hexahedron is likely to be the best choice, since equally sized hexahedrons with relatively a simple topological structure can fill the space completely. Similarly, a generalized octahedron is also a suitable choice. In general, MCs can be any shape in Fig. 4-1 and even other possible irregular solids, if appropriate weight functions can be implemented.

Tetrahedron	Hexahedron Or Cube	Octahedron	Dodecahedron	Icosahedron
				

Fig. 4-1 Five convex regular polyhedral (Platonic solids) [Atiyah *et al.* (2003)]

Furthermore, the NMM is based on the incremental method which is capable of analyzing large deformation and displacement. The simplex integration method can obtain accurate integration for any arbitrary shape [Li *et al.*, 2005]. Consequently, the governing equation for the NMM incremental step is feasible when the interpolation function in a global Cartesian system for any arbitrary shape can be built. Obviously, hexahedron or octahedron therefore is not the best choice for MC in the 3-D NMM. Moreover, the general tetrahedron is able to be considered as an ideal unit cell to form the manifold element in 3-D, referring back to the integration accuracy.

Similar to case of the 2-D NMM, the background node is the star of a MC, which could be any geometry significance point in the cover or so called center of gravity. When use trahedron manifold element, four MCs are required to overlap in order to create one manifold element. As all know, any shaped convex polygon can be decomposed into several triangles. Similar to this 2-D situation, any 3-D convex polyhedron can also be decomposed into several tetrahedrons. Moreover, there are numberless ways to decompose the 3-D convex polyhedron, by choosing different block sizes. Thus the way to decompose it determines the shape of the MCs. As it is shown in Fig. 4-2, a hexahedron can be decomposed into 6 Tetrahedrons (Fig. 4-2a), 5 Tetrahedrons (Fig. 4-2b and Fig. 4-2c) or 24 Tetrahedrons (Fig. 4-2d).

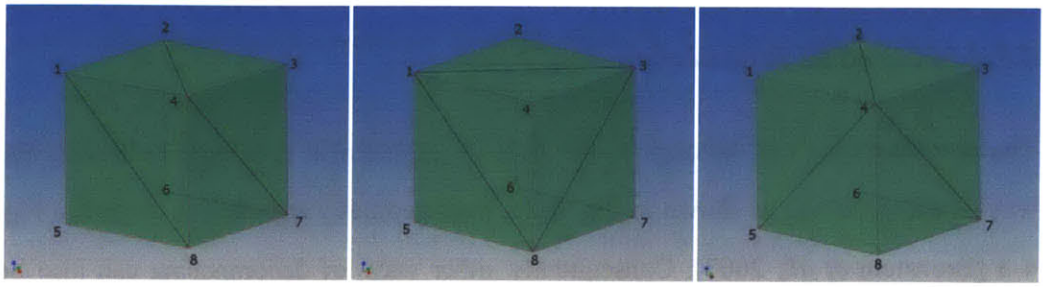

(a) (b) (c)

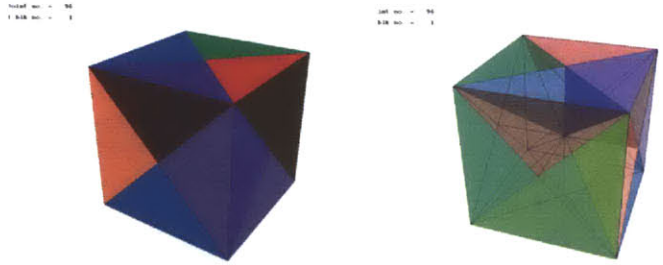

(d)

Fig. 4-2 Decomposition plan from hexahedron to tetrahedron

The way as shown in Fig. 4-2a, is not the only way to decompose it into 6 Tetrahedrons, however the advantage is that the cube divided by the way shown has the characteristic of center-symmetry. Thus, it is capable to build up the entire 3-D space without rotation. As shown in Fig. 4-2b and Fig. 4-2c, the two ways of decomposing the cube into 5 Tetra-plan are usually coupled and applied as a mixed-discretization (M-D) zone [Itasca Consulting Group, 2003]. These two kinds of mesh can overlap at the same position to decrease the strain instability disturbed by choosing mesh direction, since they are symmetric to each other. Two 'anisotropy' mathematical covers generate one cubic domain and cover, where is another extension of the manifold concept. When taking the centers of cube and 6 faces as auxiliary points, a cube can be decomposed into 24 different tetrahedrons. Moreover, the mathematical mesh has extremely symmetrical characteristic by the way of decomposing it into 24-tetrahedron.

4.1.2 MC and its formulation

The corresponding MC belongs to the field of geometrical topology. Following the way of decomposing as shown in Fig. 4-2b, their geometry structure is shown in Fig. 4-3 [Bronstein *et al.,* 2007]. Consequently, other ways of decomposing can also be found to obtain a cover structure.

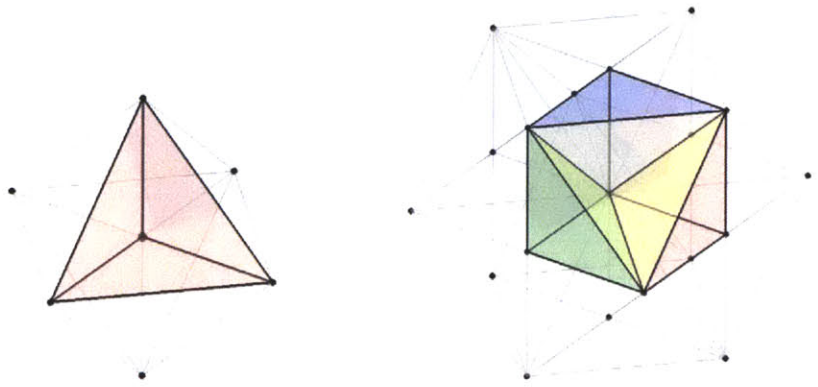

a) Cover Type I b)Cover Type II

Fig. 4-3 Configuration of MC in 3D view

a) Weight Function:

As shown in Fig. 4-3, four overlapping MCs, one type-I and three type-II covers have a common area E which is a complete tetrahedron element. Moreover, the displacement functions $u(x, y, z)$, $v(x, y, z)$ and $w(x, y, z)$ for the common area E, can be obtained by taking the weighted average of the four cover functions, which satisfy the basic NMM equation, Eq. (2-1b).

b) Cover Function:

The cover displacement functions can be a constant, and linear or even higher order polynomials or locally defined series. The expression of the cover function is

$$\boldsymbol{U}_i = \sum_{j=1}^{m} \begin{bmatrix} f_{ij}(x,y,z) & & \\ & f_{ij}(x,y,z) & \\ & & f_{ij}(x,y,z) \end{bmatrix} \begin{Bmatrix} d_{i,3j-2} \\ d_{i,3j-1} \\ d_{i,3j} \end{Bmatrix} = \boldsymbol{F}_i \boldsymbol{d}_i \tag{4-1}$$

Furthermore, the displacement for the common area is expressed as:

$$\boldsymbol{U} = \sum_{i=1}^{q} \varphi_i(x,y,z) \boldsymbol{U}_i \tag{4-2}$$

where q is the sum of the mathematical covers for an element (CE).

By substituting Eq. (4-1) into Eq. (4-2), displacement function is obtained as the following:

$$\boldsymbol{U} = \boldsymbol{\phi F d} = \boldsymbol{N d} \tag{4-3}$$

c) Constant Cover Function

A constant cover function is expressed as:

$$\boldsymbol{U}_i = \begin{Bmatrix} u(x,y,z) \\ v(x,y,z) \\ w(x,y,z) \end{Bmatrix} = \begin{bmatrix} 1 & & \\ & 1 & \\ & & 1 \end{bmatrix} \begin{Bmatrix} d_{i1} \\ d_{i2} \\ d_{i3} \end{Bmatrix} = \boldsymbol{F d}_i \tag{4-4}$$

Then,

$$\boldsymbol{N}_i = \begin{bmatrix} \varphi_i & & \\ & \varphi_i & \\ & & \varphi_i \end{bmatrix} \tag{4-5}$$

It indicates that the constant cover displacement functions generate linear displacement variation in the complete element, and it is the same as that of a tetrahedron element in the FEM.

d) Linear Cover Function

A linear cover displacement function is expressed as

$$\boldsymbol{U}_i = \begin{Bmatrix} u(x,y,z) \\ v(x,y,z) \\ w(x,y,z) \end{Bmatrix} = \begin{bmatrix} 1 & & & x & & & y & & & z & & \\ & 1 & & & x & & & y & & & z & \\ & & 1 & & & x & & & y & & & z \end{bmatrix} \begin{Bmatrix} d_{i1} \\ d_{i2} \\ d_{i3} \\ d_{i4} \\ d_{i5} \\ d_{i6} \\ d_{i7} \\ d_{i8} \\ d_{i9} \\ d_{i10} \\ d_{i11} \\ d_{i12} \end{Bmatrix} = \boldsymbol{F}\boldsymbol{d}_i \tag{4-6}$$

Then,

$$\boldsymbol{N}_i = \begin{bmatrix} \varphi_i & 0 & 0 \\ 0 & \varphi_i & 0 \\ 0 & 0 & \varphi_i \end{bmatrix} \cdot \begin{bmatrix} 1 & 0 & 0 & x & 0 & 0 & y & 0 & 0 & z & 0 & 0 \\ 0 & 1 & 0 & 0 & x & 0 & 0 & y & 0 & 0 & z & 0 \\ 0 & 0 & 1 & 0 & 0 & x & 0 & 0 & y & 0 & 0 & z \end{bmatrix}, \quad i = 1 \sim q \tag{4-7}$$

From above expressions, the NMM can exactly reduce to the standard FEM, if the following conditions are satisfied [Terada *et al*, 2003]:

a) Cover functions of physical covers are constant which is equivalent to the unknowns of the nodes in the FEM, Eq. (4-4), and the weight functions are conducted based on the (bi-)linear shape functions of the FEM;

b) Physical features including internal discontinuities, such as cracks, material interfaces, and external boundaries do not intersect with the cover-based elements.

c) On the other hand, if one discrete block is exactly one manifold element with a linear cover function like shown in Eq. (4-7), the NMM will be exactly the DDA.

4.2 GENERAL FORMULATIONS OF NMM APPROXIMATION

4.2.1 Weak form of governing equations

The weak form of the governing equation is derived by using the widely known principle of virtual work. Furthermore, the virtual work done by external forces is equal to the virtual strain energy of the system, which can be expressed as the corresponding weak form

$$\int_{\Omega} \delta\, \boldsymbol{\varepsilon}^T \boldsymbol{\sigma} dV = \int_{\Omega} \delta \mathbf{u}^T \mathbf{b} dV + \int_{\Gamma_t} \delta \mathbf{u}^T \bar{\mathbf{t}} d\Gamma - \int_{\Omega} \delta \mathbf{u}^T \rho \ddot{\mathbf{u}} dV \qquad (4\text{-}8)$$

where $\boldsymbol{\varepsilon}$ is the strain tensor; $\boldsymbol{\sigma}$ is the stress tensor; $\mathbf{u}$ is the displacement vector; $\mathbf{b}$ is the body force per unit volume; $\bar{\mathbf{t}}$ is the traction prescribed on the corresponding boundary; ρ is the density; $\ddot{\mathbf{u}}$ is the acceleration vector.

The increment approach is commonly adopted in the dynamic analysis. For the increment approach, the total-time is decomposed into a finite number of time steps. Moreover, variables, such as displacement, velocity and acceleration, are known at the beginning time t_n of the current step, and the increments of the variables during the current time step $t_n \sim t_{n+1}$ are the unknowns which need to be solved. Hence, the incremental form for the principle of virtual work is essentially needed. Energy status at t_n and t_{n+1} are both satisfied in Eq. (4-8). The incremental form is obtained by subtracting two energy equations at t_n and t_{n+1} , with ignoring the higher order terms.

$$\int_V \delta\, \Delta\boldsymbol{\varepsilon}^T \Delta\boldsymbol{\sigma} dV - \int_{\Omega} \delta\, \Delta\mathbf{u}^T \Delta\mathbf{b} dV - \int_{\Gamma_t} \delta\, \Delta\mathbf{u}^T \Delta\bar{\mathbf{t}} d\Gamma + \int_{\Omega} \delta\, \Delta\mathbf{u}^T \rho \Delta\ddot{\mathbf{u}} dV = 0 \qquad (4\text{-}9)$$

4.2.2 NMM interpolations

For a cover-based element, the NMM interpolation follows Eq. (4-3). The strain is written as:

$$\boldsymbol{\varepsilon} = \mathbf{LNd} = \mathbf{Bd} \tag{4-10}$$

Where the reduced form $\mathbf{B} = \mathbf{LN}$ is the strain matrix; $\mathbf{L}$ is the differential operator matrix.

The constitutive relation is:

$$\boldsymbol{\sigma} = \mathbf{DLNd} = \mathbf{Sd} \tag{4-11}$$

where the reduced form $\mathbf{S} = \mathbf{DLN}$ is the stress matrix.

Eq. (4-3) can be re-expressed in the incremental form:

$$\Delta\mathbf{u} = \mathbf{N}\Delta\mathbf{d} \tag{4-12}$$

Thus, the incremental strain is written as:

$$\Delta\boldsymbol{\varepsilon} = \mathbf{LN}\Delta\mathbf{d} = \mathbf{B}\Delta\mathbf{d} \tag{4-13}$$

The constitutive relation in the incremental form is

$$\Delta\boldsymbol{\sigma} = \mathbf{DLN}\Delta\mathbf{d} = \mathbf{S}\Delta\mathbf{d} \tag{4-14}$$

4.2.3 Discrete equations

Discrete equations of the dynamic analysis can be derived from Eq. (4-9) at the element level and the arbitrariness of variation $\delta\{\Delta\mathbf{d}\}$.

$$\mathbf{K}\Delta\mathbf{d} + \mathbf{M}\Delta\ddot{\mathbf{d}} = \Delta\mathbf{F} \tag{4-15}$$

The stiffness matrix $\mathbf{K}$, mass matrix $\mathbf{M}$ and the incremental load $\Delta\mathbf{F}$ at the current time step are as:

$$\mathbf{K} = \int_{\Omega} \mathbf{B}^T\mathbf{DB}dV \tag{4-16}$$

$$\mathbf{M} = \int_{\Omega} \rho\mathbf{N}^T\mathbf{N}dV \tag{4-17}$$

$$\Delta\mathbf{F} = \int_{\Omega} \mathbf{N}^T\Delta\mathbf{b}dV + \int_{\Gamma_t} \mathbf{N}^T\Delta\bar{\mathbf{t}}d\Gamma \tag{4-18}$$

It indicates that the stiffness and mass matrices are symmetric from Eq. (4-19) and Eq. (4-20). Moreover, they are also banded and sparse due to the local properties of the MC weight functions. These properties are inherited from the FEM, since it is using of the element.

For the dynamic analysis, the acceleration and the velocity can also be written by using the Newmark scheme,

$$\begin{aligned}\mathbf{d}_{n+1} &= \mathbf{d}_n + \Delta t\dot{\mathbf{d}}_n + \frac{(\Delta t)^2}{2}\left((1-2\beta)\ddot{\mathbf{d}}_n + 2\beta\ddot{\mathbf{d}}_{n+1}\right) \\ \dot{\mathbf{d}}_{n+1} &= \dot{\mathbf{d}}_n + \Delta t\left((1-\gamma)\ddot{\mathbf{d}}_n + \gamma\ddot{\mathbf{d}}_{n+1}\right)\end{aligned} \tag{4-19}$$

, and γ and β are two constants.

Then,

$$\Delta\ddot{\mathbf{d}} = \frac{1}{\beta(\Delta t)^2}\left(\Delta\mathbf{d} - \Delta t\dot{\mathbf{d}}_n - \frac{(\Delta t)^2}{2}\ddot{\mathbf{d}}_n\right) \tag{4-20}$$

Applying the scheme of the average acceleration, namely $\beta = 1/4$ and $\gamma = 1/2$, Eq. (4-20) becomes

$$\Delta\ddot{\mathbf{d}} = \frac{4}{(\Delta t)^2}\Delta\mathbf{d} - \frac{4}{\Delta t}\dot{\mathbf{d}}_n - 2\ddot{\mathbf{d}}_n \tag{4-21}$$

Substituting Eq. (4-21) into Eq. (4-15), it becomes

$$\bar{\mathbf{K}}\Delta\mathbf{d} = \Delta\bar{\mathbf{F}} \tag{4-22}$$

, and equivalent stiffness matrix $\bar{\mathbf{K}}$ and the equivalent loading vector $\Delta\bar{\mathbf{F}}$ are as:

$$\bar{\mathbf{K}} = \mathbf{K} + \frac{4}{(\Delta t)^2}\mathbf{M} \tag{4-23}$$

$$\Delta\bar{\mathbf{F}} = \Delta\mathbf{F} + \frac{4}{\Delta t}\mathbf{M}\dot{\mathbf{d}}_n + 2\mathbf{M}\ddot{\mathbf{d}}_n \tag{4-24}$$

The system matrices are formed by assembling the element matrices together, and the

unknowns attached to physical cover can be solved.

For the above steps, the discrete equations are derived in a dynamic analysis. Similarly, for a static analysis, discrete equations can also be derived by removing the inertia term in Eq. (4-8).

4.3 THREE-DIMENSIONAL BLOCK CUTTING ALGORITHM

The analysis and display of block geometry configuration are the basics for the engineering application of the NMM algorithm. Due to the complexity of rock mass geology, it is essentially necessary to develop a block cutting algorithm suitable for the NMM algorithm. Here, a geometrical cutting algorithm for 3-D block generation based on the block theory [Goodman *et al.* (1985), Shi (2006)] is proposed. The proposed algorithm is able to satisfy all the requirements for generating both the physical blocks and mathematical elements. Moreover, the description on the special loops can get information of each block during the generation of block, which satisfies the requirement of the 3-D NMM.

4.3.1 Definition of 'dip' and 'dip direction'

In the field of geological engineering, crack, joints and faultage are represented by the geological map or joint map. The underground rock masses are cut into many finite blocks. Moreover, the most fundamental information is the description of each joint plane's orientation. A modest number of joint sets is collected, whose average orientation is described by two parameters: the dip and the dip direction. In Fig. 5-4, it illustrates the terms and their relations with the geological quantities, such as strike and dip. Also, the inclined plane, shadowed in the figure, intersects with the horizontal XY plane along the strike line and plunges most steeply in the dip direction which is perpendicular to the strike line. The horizontal angle β from y toward x

defines the dip direction, and the dip is measured by the vertical angle α which is between the dip direction and the trace of the joints in a horizontal plane.

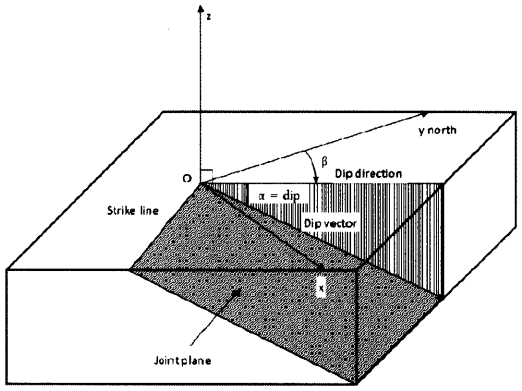

Fig. 4-4 Terms describing the attitude of an inclined plane: α, dip angle from horizontal; β, dip direction (clockwise from north)[Goodman *et al.* (1985)]

4.3.2 Single block cutting

The blocks created by the intersections of joint planes are with various shapes, and most of these blocks will have more than four faces. To illustrate it, considering a three-dimensional block with n faces formed by portions of n planes. Each plane *i* divides the whole 3-D space into an upper half-space U_m and a lower half-space L_m. The dimensions and morphology of the block system is determined by the intersection of these half-spaces for each plane, where *i=1 to n*. The steps are illustrated as follow:

(1) Firstly, choosing three faces arbitrarily from n faces, examines whether they have intersections, and then determines the coordinate of all intersections if they exist. These intersections will probably be the vertex of the generated block.

(2) To eliminate some intersection points those do not belong to the block by using the half-space judgment. Coordinates of a candidate-real-corner X_{ijk}, Y_{ijk} and Z_{ijk} should satisfy the following conditions:

$A_m X_{ijk} + B_m Y_{ijk} + C_m Z_{ijk} \geq D_m$ if the block is defined with U_m,

or

$A_m X_{ijk} + B_m Y_{ijk} + C_m Z_{ijk} \leq D_m$ if the block is defined with L_m.

(3) According to the rule that a face should have 3 vertexes at least, to determine which faces belong to the given block. Then to exclude the candidate faces which contain less than 3 vertexes.

(4) To determine all edges of the block, where a real edge is a line between a pair of real vertexes which belong to two sharing faces.

(5) To sequentially Search each face and its boundary edges. Make sure that each true face has a complete loop determination.

For instance, three generated blocks with various shapes are shown in Fig. 4-5 below.

(a) (b) (c)

Fig. 4-5 Examples of single target block cutting for different input data formats

4.3.3 Topological structure of a block system

The intersection of planes generates the outside boundaries of a single block, meanwhile produces a block system with a number of joints or joint sets inside the regarding domain. All the joints or joint sets which are cutting through the domain must be specified in order to determine the block system. Moreover, when given a set of parallel joints, the dip, dip direction and the spacing of the joints set must also be given. During this second stage of cutting, an appropriate topological structure which is representing each sub-polyhedron is required.

In the previous statement, the polyhedron is formed by a set of oriented faces and vertexes. The components of subset of the polyhedron are points, edges, and faces. Consequently, the topological information of a polyhedron is presented by the geometric information including location, geometric size, and the orientation to the subsets of the block; and the topological relationship with these subsets.

It is essentially necessary to get the geometrical information and the topological information in order to describe a polyhedron completely. A series of faces which form the block and body material index number is able to represent a complete block. Furthermore, each of the faces has a face-equation with a half-space index and a material index number. The loop components of each face are consisting of a series of vertices in some certain sequence. Moreover, supplementary information such as the volume of block, total number of vertices and the total number of faces is also provided.

4.3.4 Block operation rules

The block operations of convex blocks are capable to create any complex non-convex polyhedral with an irregular shape. For instance, the '+' block operation indicates an addition of more blocks, while the '-' block operation represents a subtraction of

blocks. Block operation can be applied to both convex and non-convex blocks [Zhang (2006)]. For further details of the basic rule of the '+' and '-' operations, when the blocks are to execute the '+' operation, their obverse facets are added, while their reverse facets are subtracted; on the other hand, when the blocks are to execute the '-' operation, their obverse facets are subtracted, while their reverse facets are added. It is known that the facet loops in the geometric structure are directional in the NMM, DDA and block theory. Even equations of the same plane still have obverse and reverse orientation properties. To illustrate it, the obverse faces refer to the circumstance where the two face equations are the same, then their direction vectors, the distance to the origin, and positions are all the same. On the other hand, the reverse faces refer to the circumstance where the absolute modules of the parameters are the same for the face equations, but the mathematical signs are reverse. Consequently, their direction vectors are opposite to each other, but the distance to the origin and positions are the same.

In Fig. 4-6, there are four generated block systems through a serious of block operations. The existing 3-D block cutting code, for instance, the 3DEC software [Itasca Consulting Group, 2003] can only produce convex blocks, and the joint polygons are assumed to cut through the target block by an infinite plane which does not terminate inside. However, the block descriptions in this proposed method do not require dividing non-convex structure into many convex shapes. Moreover, by applying the block operations, the block cutting system in this proposed method is not limited with convex blocks only.

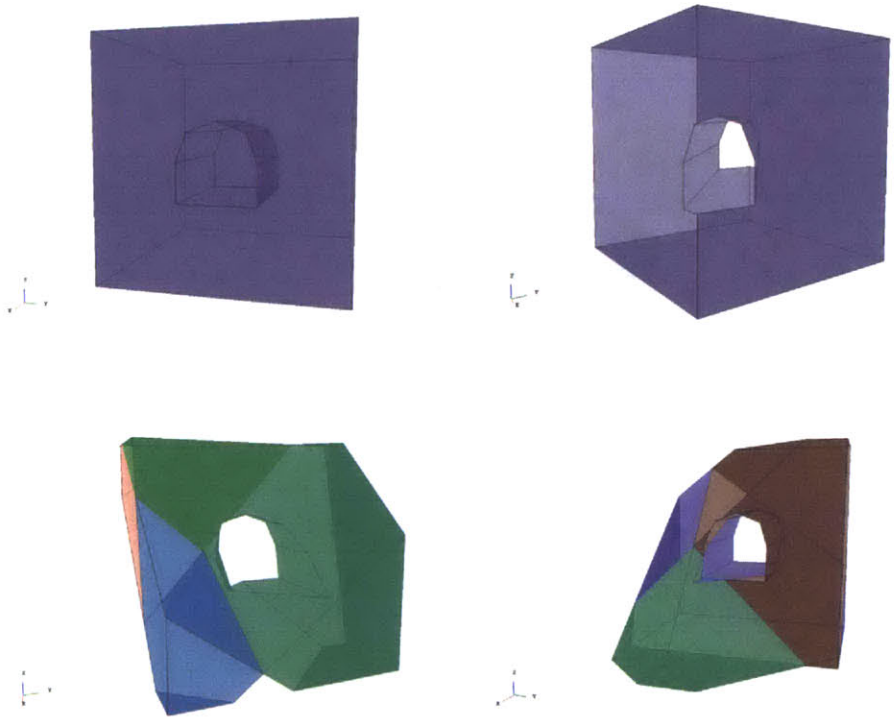

Fig. 4-6 Description to any arbitrary structure or block system

4.4 ILLUATRATION EXAMPLES

4.4.1 Movement of a free falling block

The first implementation of the 3-D NMM is to simulate the free-falling process of a single block. In Fig. 4-7, the topography of the single block in the 3-D space is defined by physical covers and mathematical covers which are introduced in the previous sections. Moreover, the cubic block falls under pure gravity. The acceleration of gravity adopted, g, is 10 m/s^2. The setup time step is 0.05s.

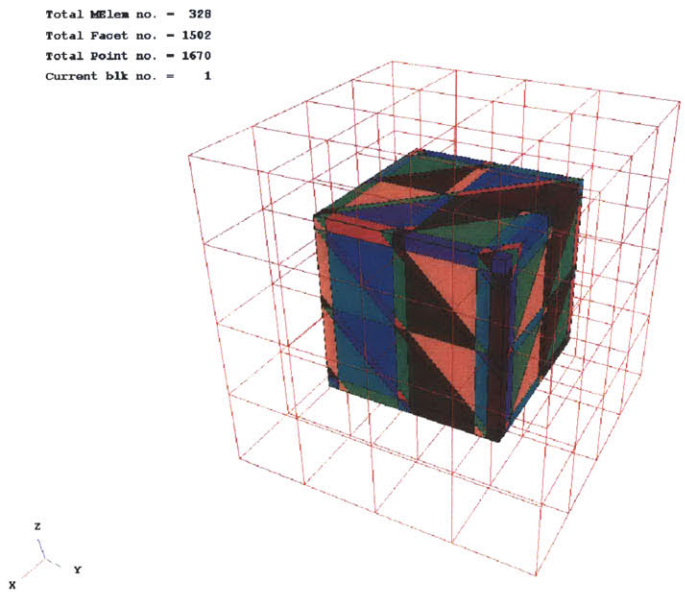

Fig. 4-7 Falling cube under gravity

Furthermore, in Fig. 4-8, it shows the comparison of NMM and exact result in terms of the displacement and velocity against time. It illustrates the reliability of the NMM, since the error of the numerical solution is less than 0.1% in the maximum absolute difference [Ma et al., 2009].

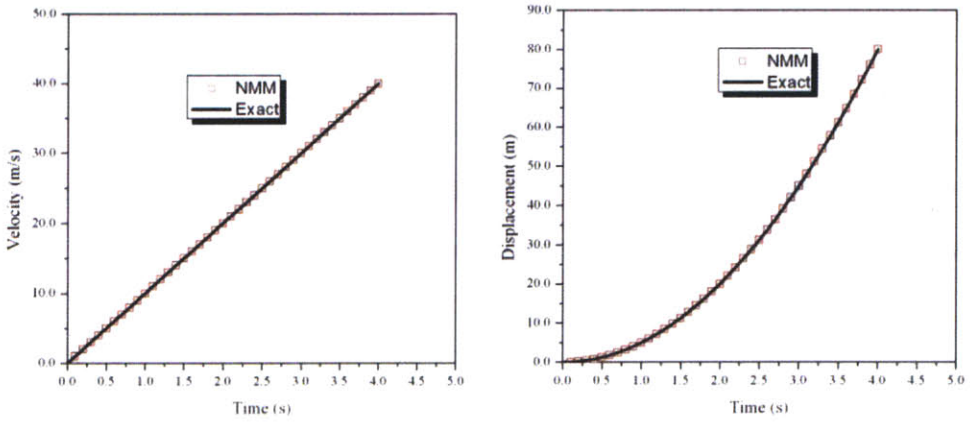

Fig. 4-8 Comparison between NMM result and exact value of displacement and velocity history

4.4.2 Effect of MC size and orientation

The advantage of NMM is that the generation of the cover based manifold elements is not restricted to the MC configurations. However, the regarding physical domain can be obtained by intersection with MCs. The following examples are aiming to investigate the effect of the MC size and the orientations of cutting planes.

A. MC size effect (quasi-static condition).

As shown in Fig. 4-9, a 2 m×2 m×0.1 m plate, with $E=10000$, $v=0.3$, $\rho=1.2$, is subjected to the gravity load ($g=10$) and fixed at four corners. The geometry of typical mesh design is shown.

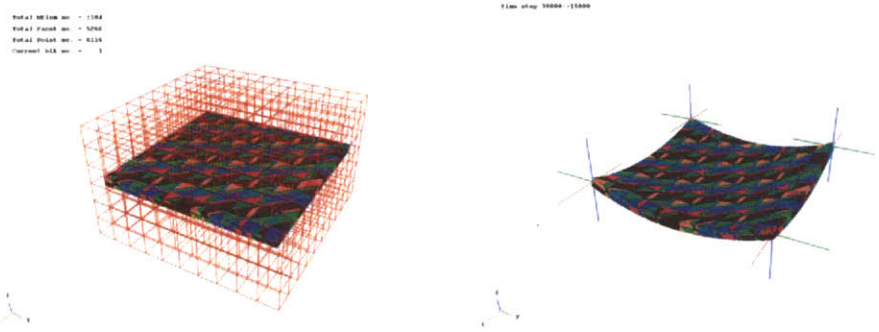

Fig. 4-9 Geometry of typical mesh design for *mesh density effect study*

In order to examine the MC size effect, six mathematical cover sizes, s= 0.52, 0.32 0.22, 0.12, 0.08, 0.05, are used. By intersecting with the physical plate, 190, 684, 1104, 3706, 8100, 19200 manifold elements are generated respectively. Moreover, the dynamical ratio is set to be 0 in order to clarify the quasi-static responses of the 6 models. Thus, the velocity of the manifold element will not be transferred to the next time step. For each case, five measurement points are set at the middle of the panel for every edge. As shown in Fig. 4-10, calculated results are converging and stable with the increase of the mesh density. Detailed results for each case are shown in Table 4-1.

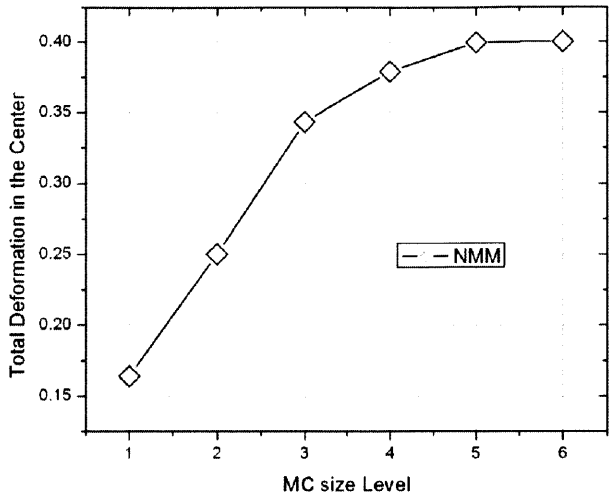

Fig. 4-10 Total Deformation Convergence test

Name	Base Solution	Refinement 1	Refinement 2	Refinement 3	Refinement 4	Refinement 5
"Total Deformation "	0.16404 m	0.25027 m [+34.45%]	0.34334 m [+27.11%]	0.37919 m [+9.45%]	0.39694 m [+4.47%]	0.39973 m [+0.76%]
Mesh properties	Spacing: 0.52 Elements: 190 Vertexes: 1156	Spacing: 0.32 Elements: 684 Vertexes: 3812	Spacing: 0.22 Elements: 1104 Vertexes: 6116	Spacing: 0.12 Elements: 3706 Vertexes: 20184	Spacing: 0.08 Elements: 8100 Vertexes: 44282	Spacing: 0.05 Elements: 19200 Vertexes: 76800

Table 4-1 Solution History at the Center of Panel

Fig. 4-11 illustrates deformation of refinement 5 at the maximum displacement time. It shows well convergence and symmetry, where M1~M4 curves present the deformation history of up, down, left and right side. Besides, the result converges to closed-form solution when mesh density increases. This property supports the validity

of the 3-D NMM calculation, since it is consistent with the FEM.

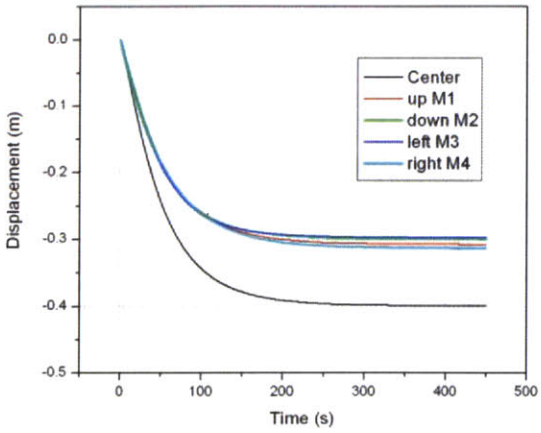

Fig. 4-11 The deformation of refinement 5 at the maximum displacement time

B. *MC orientation effect (dynamic condition).*

Now, the same plate is subjected to a constant point load $L=5$ at the center. In order to investigate the dynamical response fully, the dynamical ratio is set as 0.999. In Fig. 4-12, two different orientations of the plate are shown.

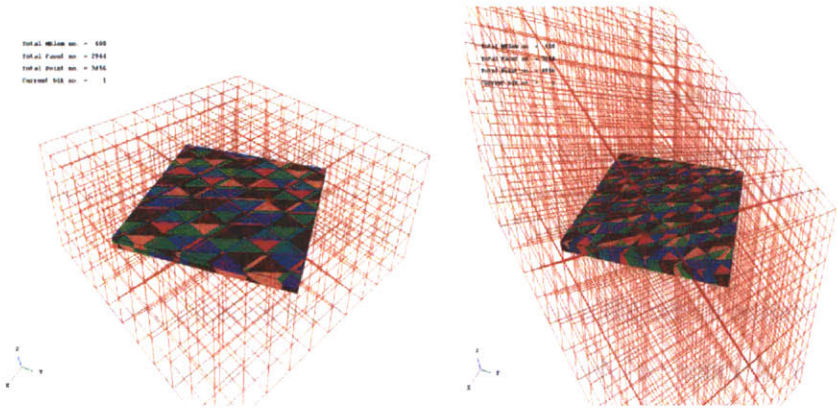

Fig. 4-12 Geometry of mesh designs for *mesh orientation effect study*

Fig. 4-13 shows the Z displacement histories of the center point. It indicates that the orientation of the MCs has negligible effect on the plate maximum displacement at center. It shows accurate and stable maximum displacement after converging, and

convergence time is about same when total element number is about same. Table 4-2 shows the detailed results.

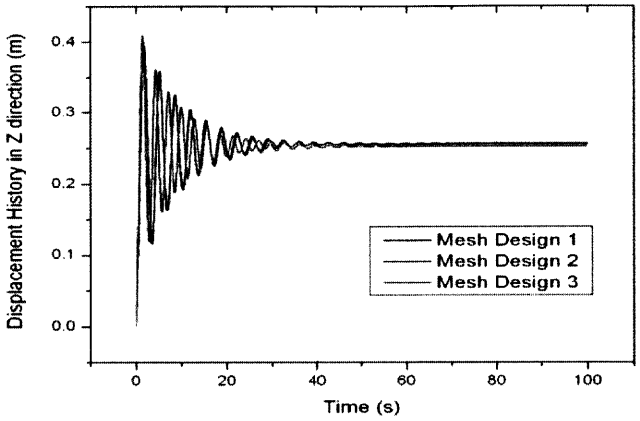

Fig. 4-13 *Z* displacement histories of center point

Name	**Mesh Design 1**	**Mesh Design 2**	**Mesh Design 3**
"Results"	Peak disp.: 0.39598 m Stable disp.: 0.255538 m Stable time: 48.86s.	Peak disp.: 0.40054 m Stable disp.: 0.252278 m Stable time: 49.16s	Peak disp.: 0.40878 m Stable disp.: 0.253667 m Stable time: 46.34s
Mesh properties	Spacing: 0.32 Elements: 684 Direction: 0 0, 90 0, 90 90	Spacing: 0.31 Elements: 608 Direction: 0 0, 90 30, 90 120	Spacing: 0.28 Elements: 618 Direction: 30 0, 90 30, 90 120

Table 4-2 Mesh design comparison

As the orientation of the MCs has little effect to the simulation result, it ensures the accuracy and efficiency of the 3-D NMM. Moreover, it also supports the validity of the 3-D NMM dynamic algorithm [Ma et al., 2009].

CHAPTER 5 SUPPORT DESIGN

5.1 SUPPORT DESIGN INVESTIGATION IN TUNNEL AND SLOPE ENGINEERING

The core thesis of block theory is on stability analysis of keyblock which this proposed method based on. In excavations, it is crucial to consider the critical blocks, namely keyblocks. The keyblock is a finite, removable, and potentially unstable block mass. Moreover, it is made up of the joints and free surfaces. To determinate whether a finite convex block removable or not depends on its shape which is relating to the excavation. Furthermore, a non-removable finite block is termed as tapered. The Necessary and sufficient conditions for determining the removability of a finite convex block are that it is removable if it has the free surfaces and its joints planes cannot make up a block.

In block theory, the relationship connecting the orientation of the resultant force and the orientation of sliding is established. Also, by obtaining other kinematic constraints and a specific orientation of the resultant force, it is able to establish which sliding mode is applicable to each block. As stated in block theory, there are three modes of sliding acting on the removable block, and the orientation and the value of the three modes of sliding are also defined.

Lifting:

$$\boldsymbol{s}=\boldsymbol{r} \qquad F=|\,\boldsymbol{r}\,| \tag{5-1}$$

Sliding on a single face:

$$\boldsymbol{s}_i=(\boldsymbol{n}_i\times\boldsymbol{r})\times\boldsymbol{n}_i/|\,\boldsymbol{n}_i\times\boldsymbol{r}\,| \qquad F=|\,\boldsymbol{n}_i\times\boldsymbol{r}\,|-|\,\boldsymbol{n}_i\cdot\boldsymbol{r}\,|\tan\phi_i \tag{5-2}$$

Sliding on two faces:

$$\boldsymbol{s}_{ij}=(\boldsymbol{n}_i\times\boldsymbol{n}_j)\,\mathrm{sign}((\boldsymbol{n}_i\times\boldsymbol{n}_j)\cdot\boldsymbol{r})/|\,\boldsymbol{n}_i\times\boldsymbol{n}_j\,| \tag{5-3}$$

$$F=[|\boldsymbol{r}\cdot(\boldsymbol{n_i}\times\boldsymbol{n_j})||\boldsymbol{n_i}\times\boldsymbol{n_j}|-|(\boldsymbol{r}\times\boldsymbol{n_j})\cdot(\boldsymbol{n_i}\times\boldsymbol{n_j})|\tan\phi_i-|(\boldsymbol{r}\times\boldsymbol{n_i})\cdot(\boldsymbol{n_i}\times\boldsymbol{n_j})|\tan\phi_j]]/|\boldsymbol{n_i}\times\boldsymbol{n_j}|^2 \quad (5\text{-}4)$$

The sliding orientation, $\boldsymbol{s_i}$, is the orthographic projection of $\boldsymbol{r}$ on plane $\boldsymbol{I}$; $\boldsymbol{s_{ij}}$ is the orientation of the intersection line of two planes $\boldsymbol{i}$ and $\boldsymbol{j}$ which makes an right angle with the orientation of the resultant force $\boldsymbol{r}$; F is the sliding forces acting on the block; ϕ_i, ϕ_j are the friction angles of joints $\boldsymbol{i}$ and $\boldsymbol{j}$ respectively; $\boldsymbol{n_i}$, $\boldsymbol{n_j}$ are the upward normal vectors to plane $\boldsymbol{i}$ and $\boldsymbol{j}$.

When the normal forces from the adjacent blocks passing through the joints and the cohesion acting on the joint planes are taken into consideration, the refinement of the orientation and the value of the three modes of sliding are shown as follow:

Lifting:

$$\boldsymbol{s}=\boldsymbol{r} \qquad F=|\boldsymbol{r}|+\sum F_l-\sum F_l*\tan\phi_l \quad (5\text{-}5)$$

Sliding on a single face:

$$\boldsymbol{s_i}=(\boldsymbol{n_i}\times\boldsymbol{r})\times\boldsymbol{n_i}/|\boldsymbol{n_i}\times\boldsymbol{r}| \quad (5\text{-}6)$$

$$F=|\boldsymbol{n_i}\times\boldsymbol{r}|-|\boldsymbol{n_i}\cdot\boldsymbol{r}|\tan\phi_i+\sum F_l-\sum F_l*\tan\phi_l - c_i*\boldsymbol{A_i} \quad (5\text{-}7)$$

Sliding on two faces:

$$\boldsymbol{s_{ij}}=(\boldsymbol{n_i}\times\boldsymbol{n_j})\text{sign}((\boldsymbol{n_i}\times\boldsymbol{n_j})\cdot\boldsymbol{r})/|\boldsymbol{n_i}\times\boldsymbol{n_j}| \quad (5\text{-}8)$$

$$F=[|\boldsymbol{r}\cdot(\boldsymbol{n_i}\times\boldsymbol{n_j})||\boldsymbol{n_i}\times\boldsymbol{n_j}|-|(\boldsymbol{r}\times\boldsymbol{n_j})\cdot(\boldsymbol{n_i}\times\boldsymbol{n_j})|\tan\phi_i-|(\boldsymbol{r}\times\boldsymbol{n_i})\cdot(\boldsymbol{n_i}\times\boldsymbol{n_j})|\tan\phi_j]]/|\boldsymbol{n_i}\times\boldsymbol{n_j}|^2+\sum F_l-\sum F_l*\tan\phi_l-c_i*\boldsymbol{A_i}-c_j*\boldsymbol{A_j} \quad (5\text{-}9)$$

$\sum F_l$ is the force from all joint planes; ϕ_l is the friction angle of joint planes; $\boldsymbol{A_i}$, $\boldsymbol{A_j}$ are the areas of joint $\boldsymbol{i}$ and $\boldsymbol{j}$ respectively; c_i, c_j are the cohesions of joint $\boldsymbol{i}$ and $\boldsymbol{j}$.

The advantage of Q-value system and RMR is that it is sufficient to cover all rock mass circumstances based on the required six parameters of a rock mass. On the other

hand, the disadvantage is that it requires exclusive value of the six parameters from one specimen or geological experts' opinions to determinate the values of the parameters, which is very inconvenient in most cases. However, block theory is apparently more advantage. Thus, the support design based on block theory only requires cohesion, friction, the dip and dip direction of joints and density of rock mass. It is relatively easy to obtain these values, and these values are also unique for an individual specimen. Besides, it is only necessary to support the unstable block identified by the block theory. Moreover, the block theory is also recommended to use in checking the traditional rock support and reinforcement design.

5.2 DISCUSSION ABOUT SUPPORT DESIGN IN SLOPE AND TUNNEL ENGINEERING

A numerical model of rock slope is shown in Fig. 5-1. After excavation the keyblocks of the rock slope engineering will slide without support, as shown in Fig. 5-2. As a consequence, all the blocks in colors will slide from the main rock mass if without the support.

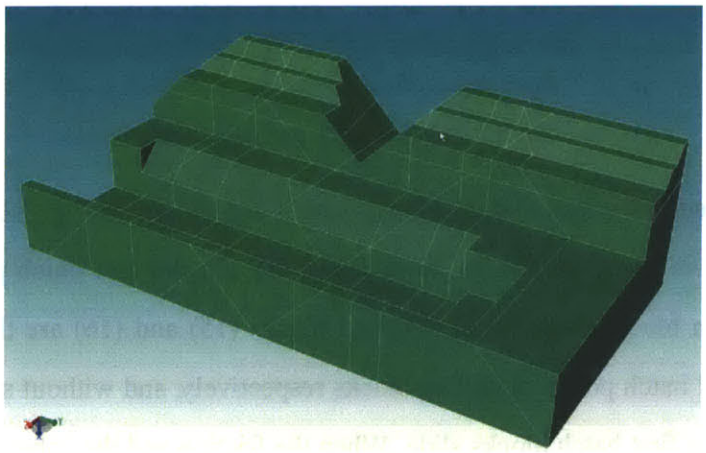

Fig. 5-1 A rock slope model

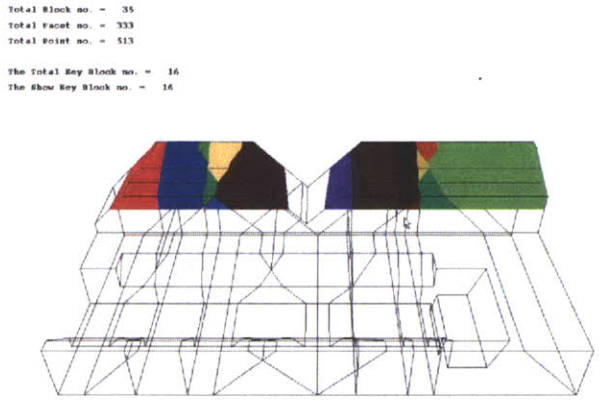

Fig. 5-2 The potential sliding blocks in the slope

As shown in Fig. 5-3, these blocks are termed as the batch time sliding blocks. Namely, when they are sufficiently supported, the overall stability of the rock slope will be fine.

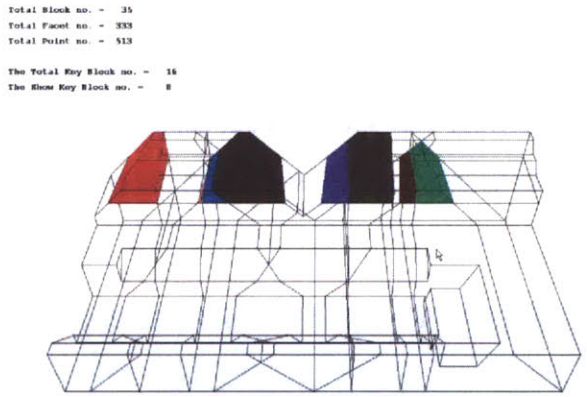

Fig. 5-3 The first batch potential sliding blocks

All the sixteen potential sliding blocks which are shown in Fig. 5-2 are illustrated individually in Fig. 5-4. Blocks, from (1) to (8), are the first batch potential sliding blocks. Then blocks from (9) to (14) and blocks (15) and (16) are the second batch and the third batch potential sliding blocks respectively, and without support they will slide after the first batch blocks slide. When the friction and the cohesion of each joint plane are equal to zero, detail results of the volume, the potential sliding force, the support pressure, the sliding orientation of blocks and the support orientation are listed in Table 5-1. Then, the overall stability of slope will be fine if it is using the

support design based on the block theory.

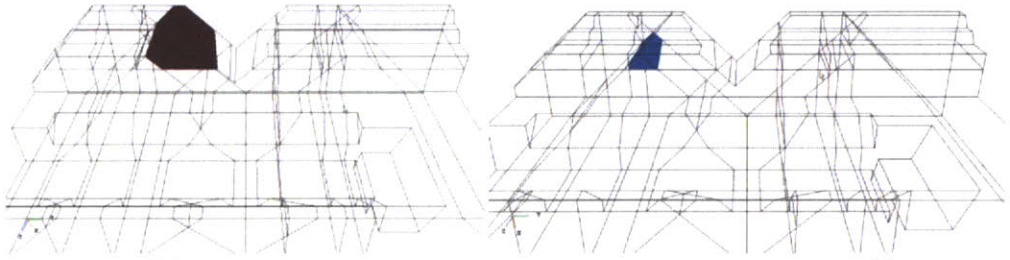

(1) (2)

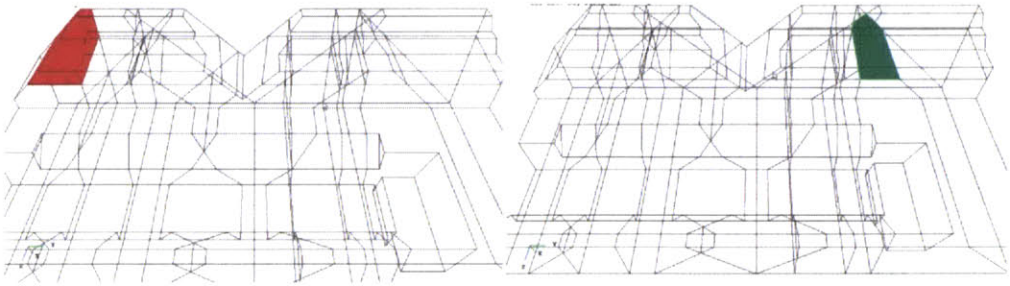

(3) (4)

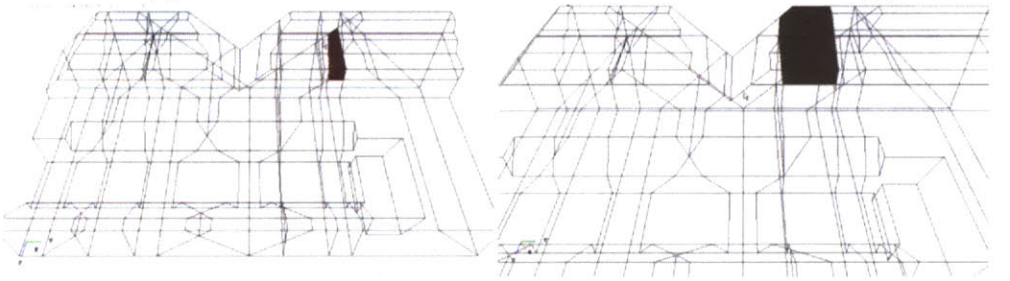

(5) (6)

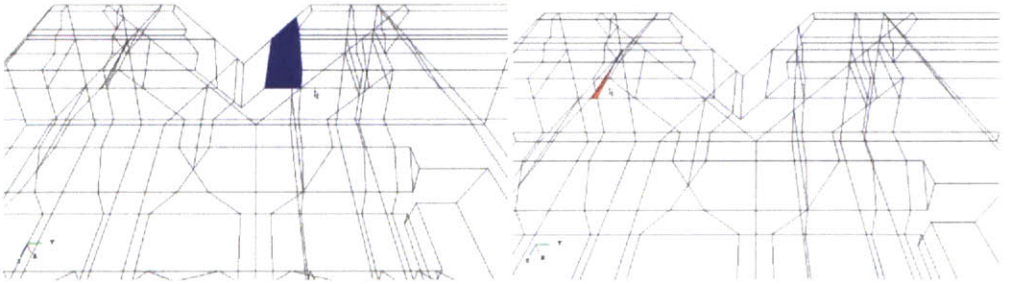

(7) (8)

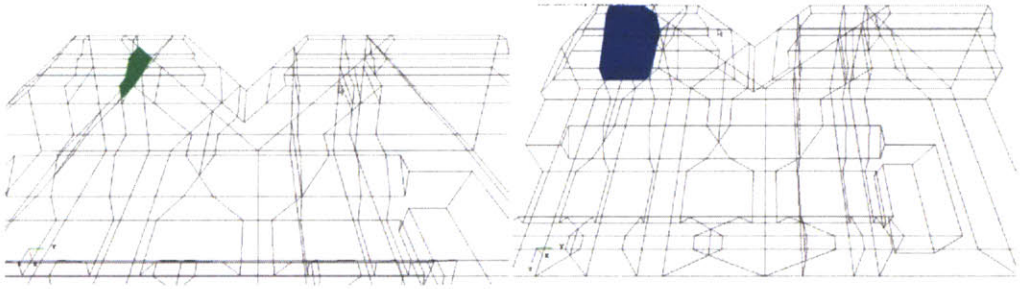

(9) (10)

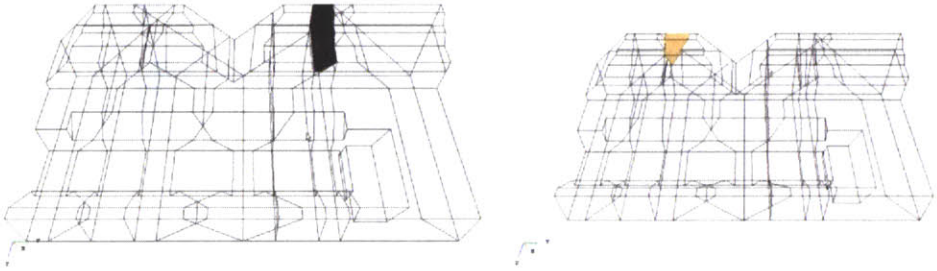

(11) (12)

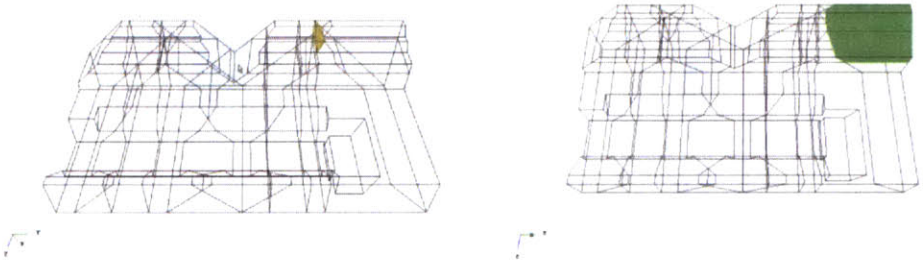

(13) (14)

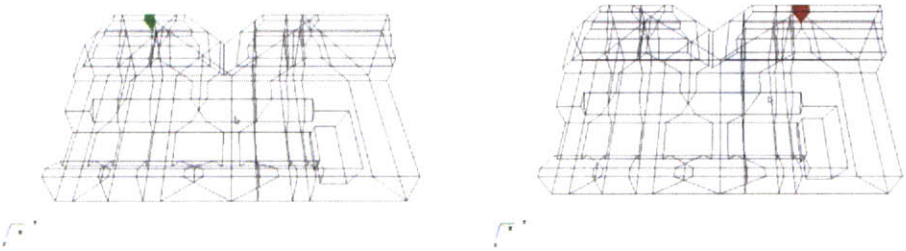

(15) (16)

Fig. 5-4 the potential sliding blocks

The number block	The sliding force(kN)	The sliding direction vector			The volume of block(m^3)	The support pressure(kPa)
1	194328	0.100	0.000	0.995	100	41981.9
2	61152	0.100	0.000	0.995	31	325276.9
3	165194	0.100	0.000	0.995	85	45249.4
4	107312	0.100	0.000	0.995	55	45249.4
5	32395	0.100	0.000	0.995	17	45249.4
6	191689	0.100	0.000	0.995	98	113430.1
7	79093	0.100	0.000	0.995	41	330564.8
8	93909	0.100	0.000	0.995	48	56599.9
9	21140	0.100	0.000	0.995	11	56599.9
10	181233	0.100	0.000	0.995	93	56599.9
11	106188	0.100	0.000	0.995	54	40848.7
12	600275	0.707	0.707	0.000	43	40848.7
13	239486	1.000	0.000	0.000	12	1738683.6
14	403603	0.100	0.000	0.995	207	18315
15	595424	1.000	0.000	0.000	30	40950.9
16	156731	1.000	0.000	0.000	8	28952.9

Table 5-1 the information of potential sliding blocks

In the calculation, density of rock mass is $2.0x10^3kg/m^3$, gravity acceleration is $9.8m/s^2$, the friction and the cohesion are zero. Then, orientation of support is represented by the vector of (0.995, -0.000, -0.100).

A numerical model of a tunnel with random joint planes is shown in Fig 5-5. As shown in Fig. 5-6, the blocks in color are the potential sliding blocks which will slide after excavation without support. Moreover, they concentrate in the top and right side of the tunnel due to the orientation of the joins.

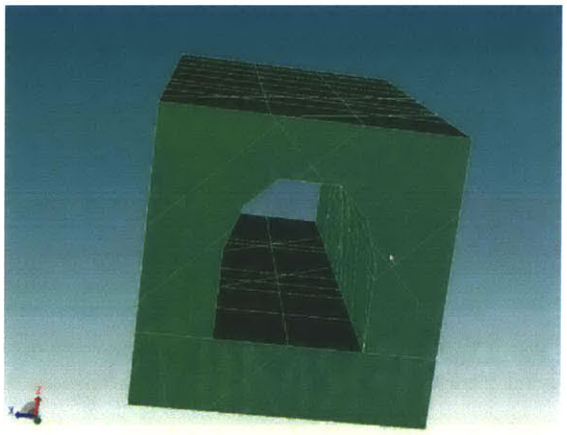

Fig. 5-5 The tunnel model

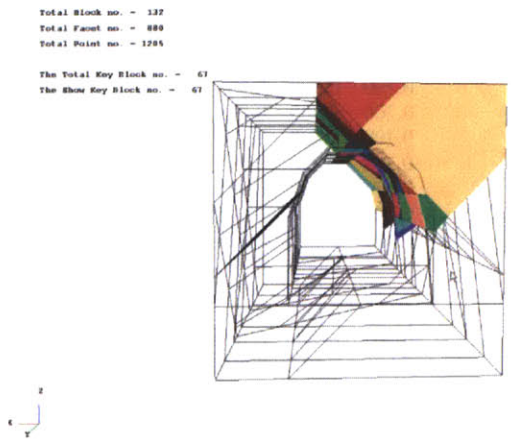

Fig. 5-6 the potential sliding block of tunnel model

In traditional approach, when the support is not sufficient to support the blocks, normally it is recommended to decrease the spacing of the rock bolts and increase the number of rock bolts for safety concern. However, it is a waste, since only keyblock are needed to be supported. On the other hand, support design based on the block theory can identify keyblocks during excavation, and it is also important to point out the essence of reinforcing the second batch by adjusting the support force acting on the keyblocks.

CHAPTER 6 THE 3D-NMM SOFTWARE APPLICATIONS AND SIMULATIONS

The functions of cutting algorithm, improved contact algorithm and support design are compelled as one integrated software, namely the proposed 3D-NMM software. So far, this is the first time that all these functions are implemented together. Both practical and illustratable examples are given, in comparison of the 3DEC software which is the currently leading software, in this chapter.

The process of generating 3-D blocks, i.e. the cutting process, is mainly based on a new proposed cutting algorithm. This proposed cutting algorithm is aiming to generate blocks from joints and free faces in a three-dimensional space.

In general, there are two cases of generating blocks. When the joints are longer than the dimension of the target block, the cutting algorithm is relatively simple, and only convex blocks are generated. On the other hand, when the joints are shorter than the dimension of the target block, the cutting algorithm becomes relatively complex due to following reasons: (1) the blocks could be concave; (2) the faces of the blocks could be concave; (3) a block could contain sub-blocks inside; (4) a block could contain holes inside; (5) the faces of blocks could contain sub-faces or holes inside.

However, most of the existing block cutting algorithms can only deal with the simple case, namely the joints are long enough and only producing convex blocks is required. Hence, it is essentially necessary to propose an improved algorithm which can describe not only convex blocks and concave blocks, but also simply connected blocks and multiply connected blocks. Some classic concave examples are shown in Fig. 6-1.

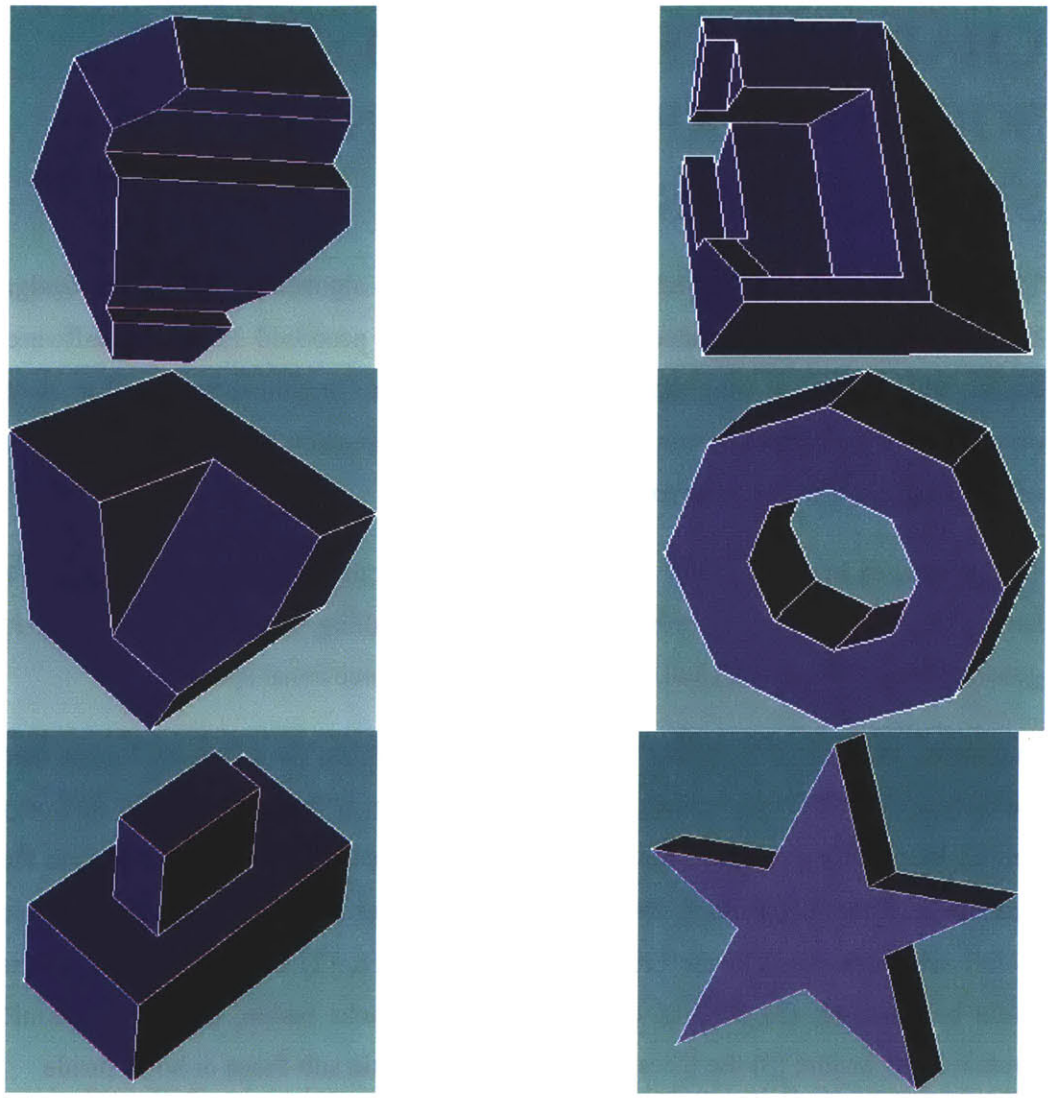

Fig. 6-1 arbitrary shaped blocks (concave blocks)

The 3DEC software is commercial software for engineering purpose which is currently leading software. However, the proposed 3D-NMM software includes all functions of 3DEC, besides, it also includes thee functions and advantages that the 3DEC software does not have. Firstly, some classic examples which are done by the 3DEC software are represented through the proposed 3D-NMM software, for comparing purposes.

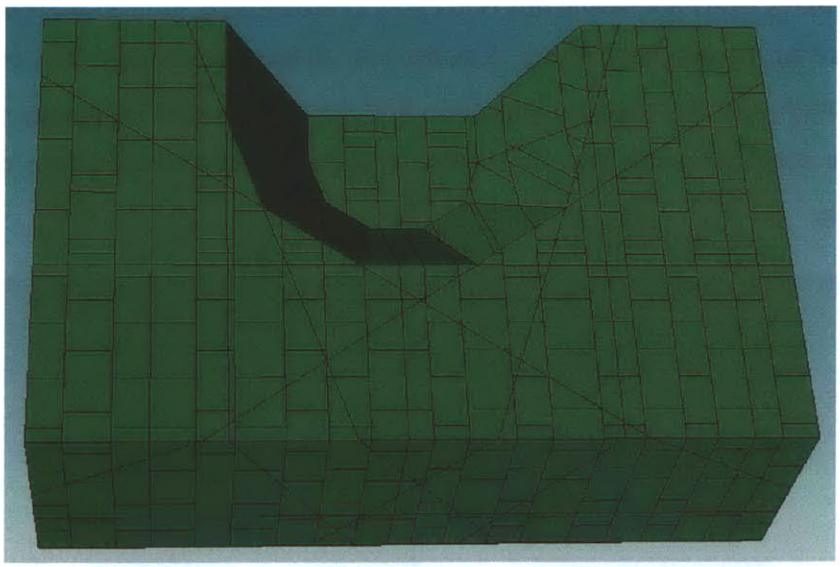

(a1)

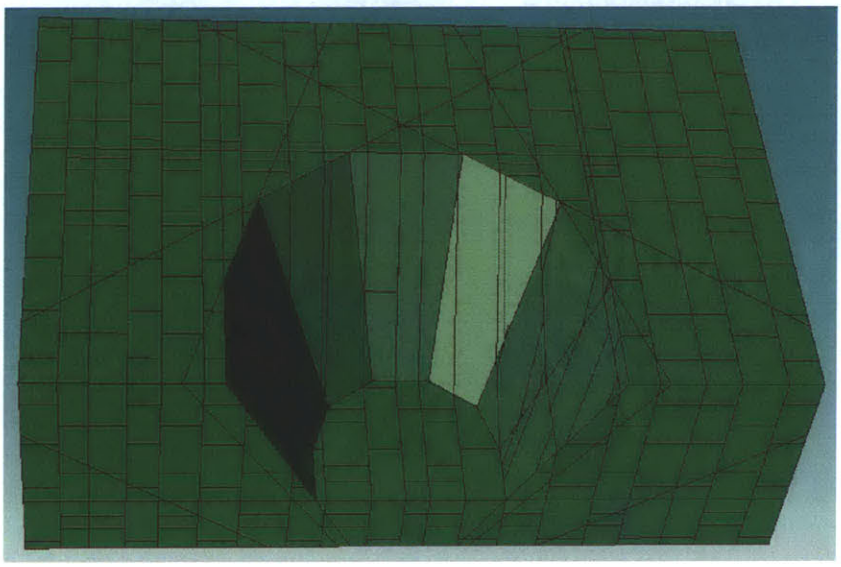

(a2)

Fig. 6-2 3D cutting open pit by 3D-NMM (a1) back view (a2) front view

'Open pit' is a classic example presented in the 3DEC software. However, it can be represented by the proposed 3D-NMM software either, as shown in Fig. 6-2. The major difference between two softwares is that the 3DEC software is using infinite planes to cut the block, i.e. each joint need to be cut through all surfaces, on the other hand, the proposed 3D-NMM software is using finitely cutting algorithm. It implies that the proposed 3D-NMM software is presenting the 3-D block in the way they are maturely are, for instance, not all joints are totally through the whole block. While the

way the 3DEC software handle this is to apply arbitrary paste force to paste the blocks, which are cut by infinitely planes, together into an integrated block. The problem is the arbitrary paste force applied may not reflect the real situation happening in field. It therefore could influence the computation result calculated based on the numerical modeling.

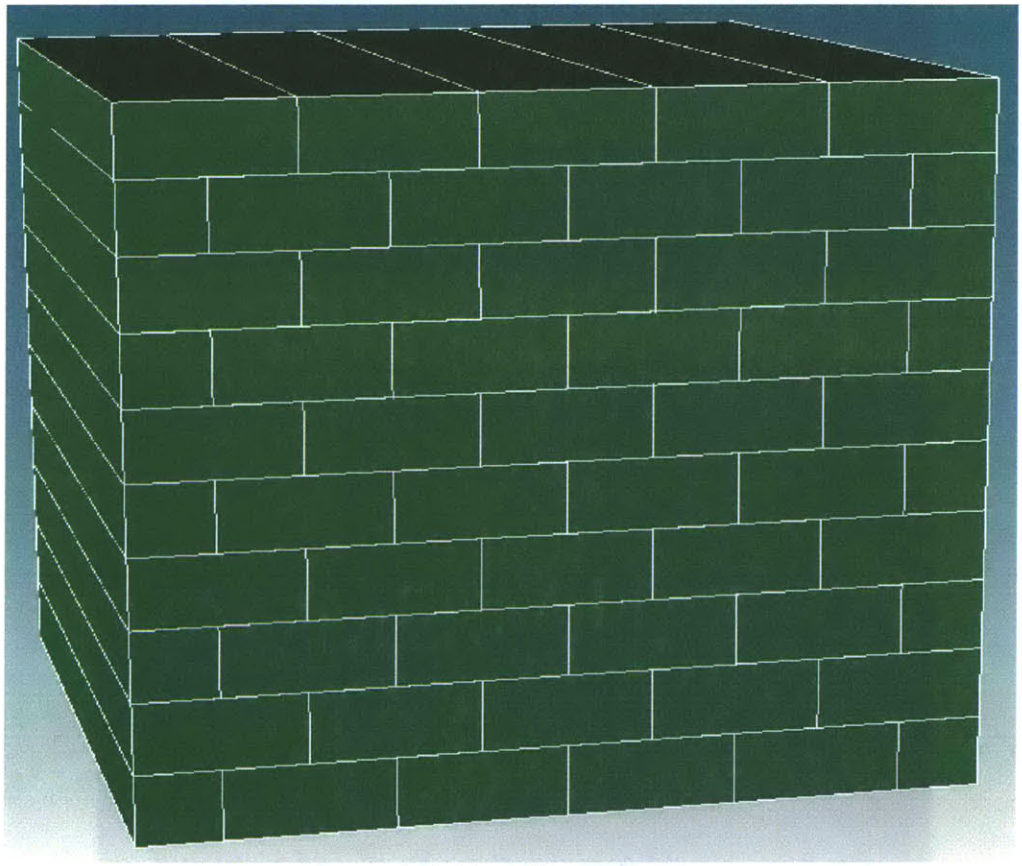

Fig. 6-3 the brick wall by 3D-NMM

Moreover, another classic example presented in the 3DEC software is 'the brick wall'. Again, it is represented in the proposed 3D-NMM software. This example illustrates another new trait in the proposed 3D-NMM software, namely the function of adding up block being cut up. This new trait enables user accomplish complicated cutting operations without disturbing the integrality of the whole block. Through this example and previous example, the advantages of the proposed 3D-NMM software comparing to the 3DEC software become prevailed. It is clearly that the proposed 3D-NMM software is more accurate and realistic than the 3DEC software in 3-D block numerical modeling.

The application of the proposed 3D-NMM software is much further than these. It can be applied in various fields, such as rock engineering, civil engineering, geology and even industrial purpose. To illustrate the strength of the proposed 3D-NMM software, various examples, such as excavation, tunnels, and even ancient miracles, are to be elaborated in the following part.

In field of civil engineering, tunnel excavation is an important engineering practice. Tunnels are commonly excavated through mountain or underground. The issue of safety is extremely vital, due to the potential of collapse. It therefore is essential that any tunnel project starts with a comprehensive investigation of rock or ground conditions. The results of the investigation will allow proper choice of machinery and methods for excavation and rock or ground support, and will reduce the risk of encountering unforeseen rock or ground conditions. However, the cost of investigation is relatively high and the accuracy is not enough. An accurate numerical modeling therefore is needed which the proposed 3D-NMM software is capable. Firstly, user needs to define a 3-D block, as shown in Fig. 6-4 (a1). Secondly, as shown in Fig. 6-4 (a2), various types of tunnel are available to be chosen by user. Finally, the numerical models are completed as shown in Fig. 6-4 (b1) to (b3). As shown in Fig. 6-4 (b1), a complex intersecting tunnel system in a jointed rock mass is simulated for analysis and engineering purpose. The proposed 3D-NMM software enables user to view of generated block in both internal view and external view, and the function of 'zoom' enables user to walk through the channel with a arbitrary camera, which is 360°free, as shown in Fig. 6-4 (a3). Besides, the function of 'texture' makes the generated 3-D block is more realistic, as shown in Fig. 6-4 (b2). Arbitrary finite discontinuities can be added in the 3-D numerical model, as shown in Fig. 6-4 (b3). With further development, geologist and engineers may be able to use the proposed 3D-NMM software to exanimate the in-situ conditions just like to be there personally.

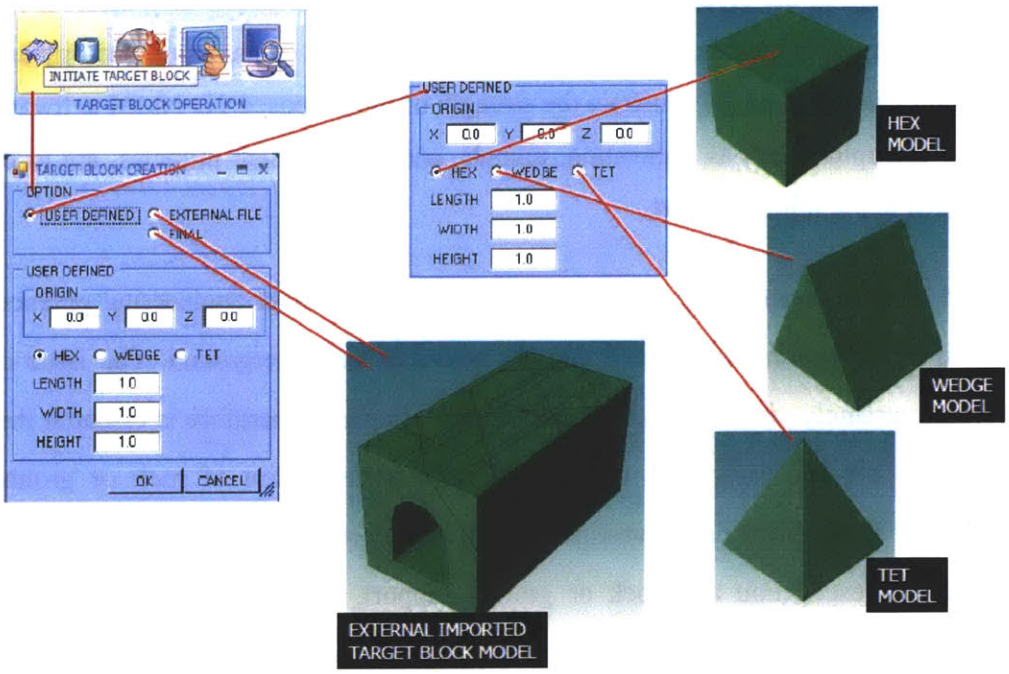
INITIATE TARGET BLOCK
TARGET BLOCK OPERATION
TARGET BLOCK CREATION
OPTION
USER DEFINED
EXTERNAL FILE
FINAL
USER DEFINED
ORIGIN
X 0.0 Y 0.0 Z 0.0
HEX WEDGE TET
LENGTH 1.0
WIDTH 1.0
HEIGHT 1.0
OK CANCEL
USER DEFINED
ORIGIN
X 0.0 Y 0.0 Z 0.0
HEX WEDGE TET
LENGTH 1.0
WIDTH 1.0
HEIGHT 1.0
HEX MODEL
WEDGE MODEL
TET MODEL
EXTERNAL IMPORTED TARGET BLOCK MODEL

(a1)

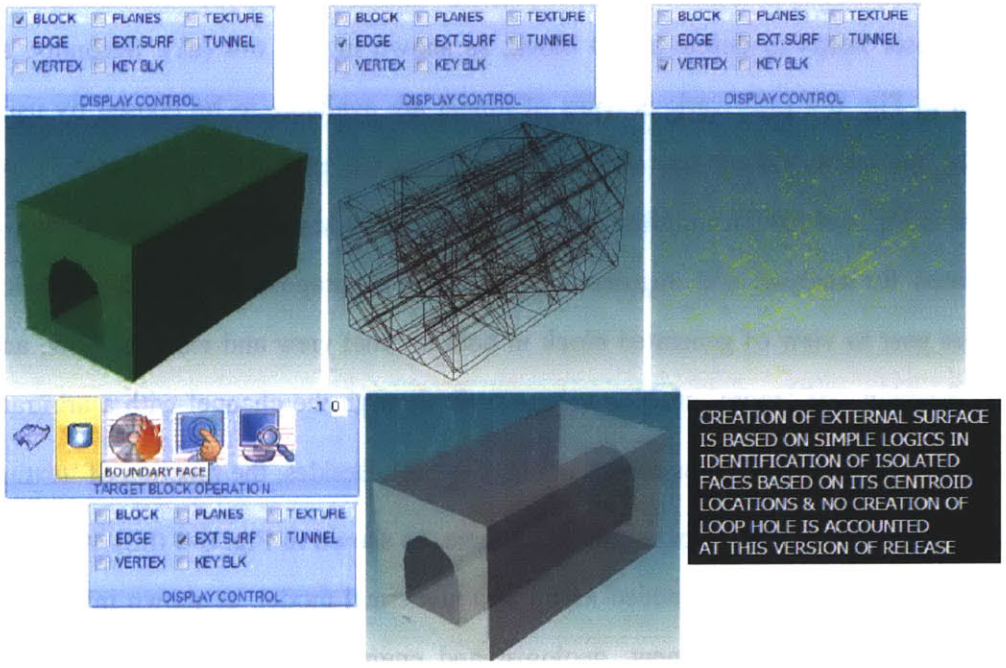
BLOCK PLANES TEXTURE
EDGE EXT.SURF TUNNEL
VERTEX KEY BLK
DISPLAY CONTROL
BLOCK PLANES TEXTURE
EDGE EXT.SURF TUNNEL
VERTEX KEY BLK
DISPLAY CONTROL
BLOCK PLANES TEXTURE
EDGE EXT.SURF TUNNEL
VERTEX KEY BLK
DISPLAY CONTROL
BOUNDARY FACE
TARGET BLOCK OPERATION
BLOCK PLANES TEXTURE
EDGE EXT.SURF TUNNEL
VERTEX KEY BLK
DISPLAY CONTROL
CREATION OF EXTERNAL SURFACE IS BASED ON SIMPLE LOGICS IN IDENTIFICATION OF ISOLATED FACES BASED ON ITS CENTROID LOCATIONS & NO CREATION OF LOOP HOLE IS ACCOUNTED AT THIS VERSION OF RELEASE

(a2)


WALK THRU
UTILITY
TILT UP
WALK FORWARD
Q W
WALK LEFT
A S D
WALK RIGHT
Z
TILT DOWN
WALK BACKWARD
SPACE BAR = CENTER SCREEN

(a3)

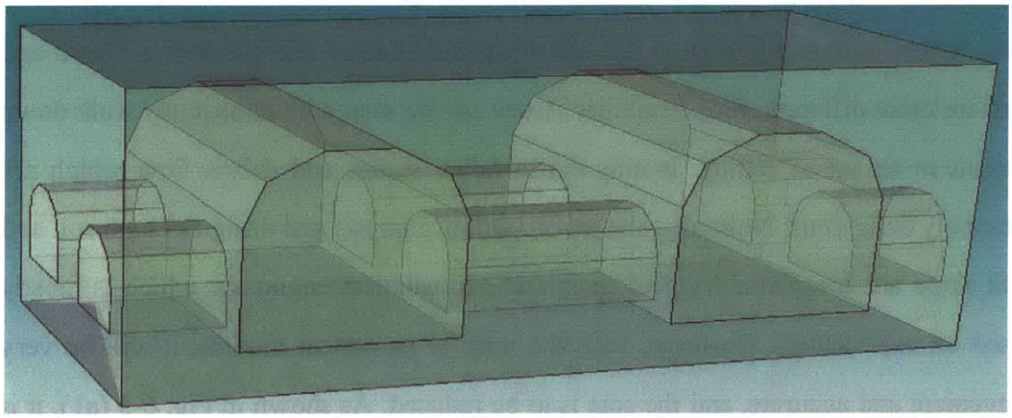

(b1)

(b2)

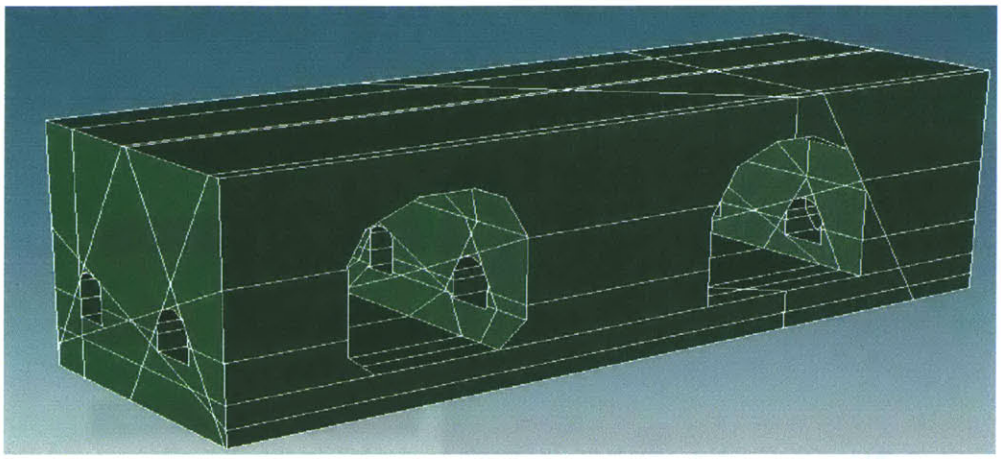

(b3)

Fig. 6-4 cutting a tunnel system in a jointed rock mass (a) cutting process (b) completed models

In the field of geology and geotechnical engineering, the analysis on slope stability is vital. Slopes commonly refer to soil and rock, and method and properties of soil and rock are quite different. Slope stability issues can be seen with almost any walk down a ravine in an urban setting. It may cause fallen stones and debris flow which are extremely dangerous. Normally, the investigation, analysis and design of both soil and rock slope are completed by geologists and geotechnical engineers, which is mostly based on experiences. However, with the help of numerical models, it will be very convenient and accurate, and the cost is to be reduced. As shown in Fig. 6-5 (a1), it is the numerical modeling of a typical rock slope generated by the proposed 3D-NMM software. Fig. 6-5 (a2) is the same rock slope with arbitrary discontinuities or can be called the model before the elements add up. Fig. 6-5 (a3) is the same numerical model with rock texture, which is through the function of 'texture', and is more realistic and vivid. On the other hand, Fig. 6-5 (b1) and Fig. 6-5 (b2) depict a typical soil slope and the same slope with texture.

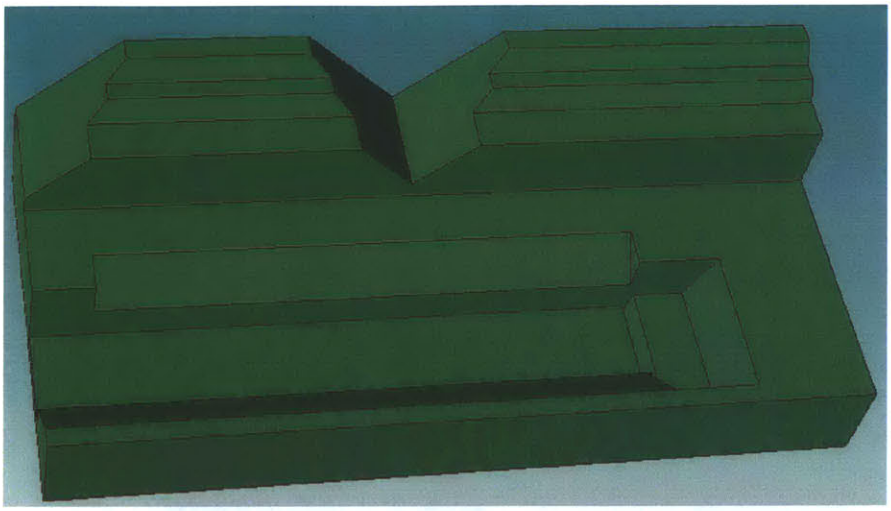

(a1)

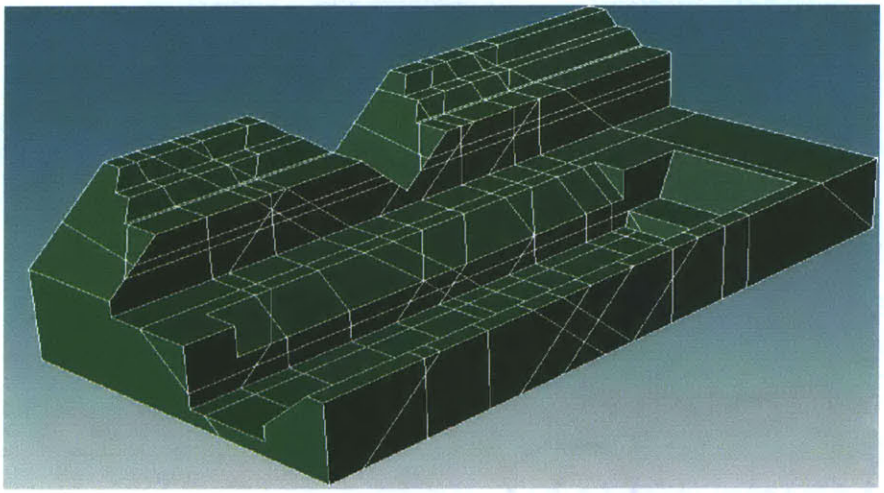

(a2)

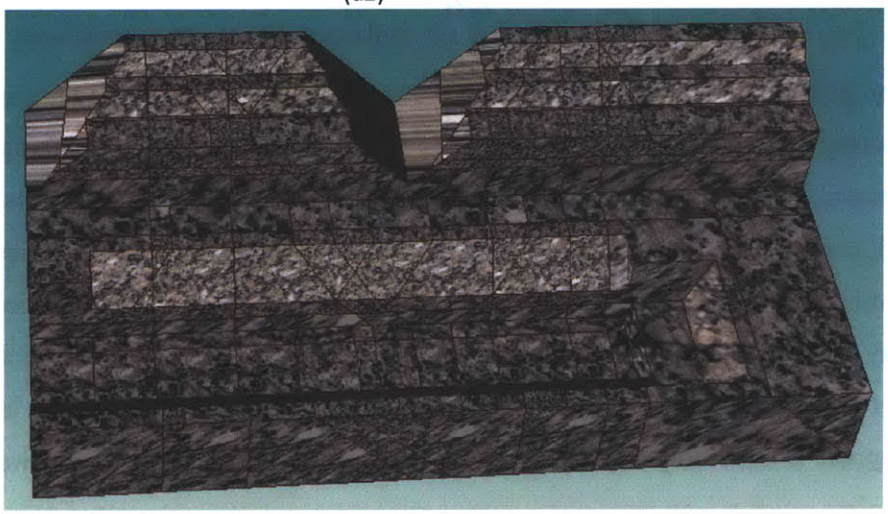

(a3)

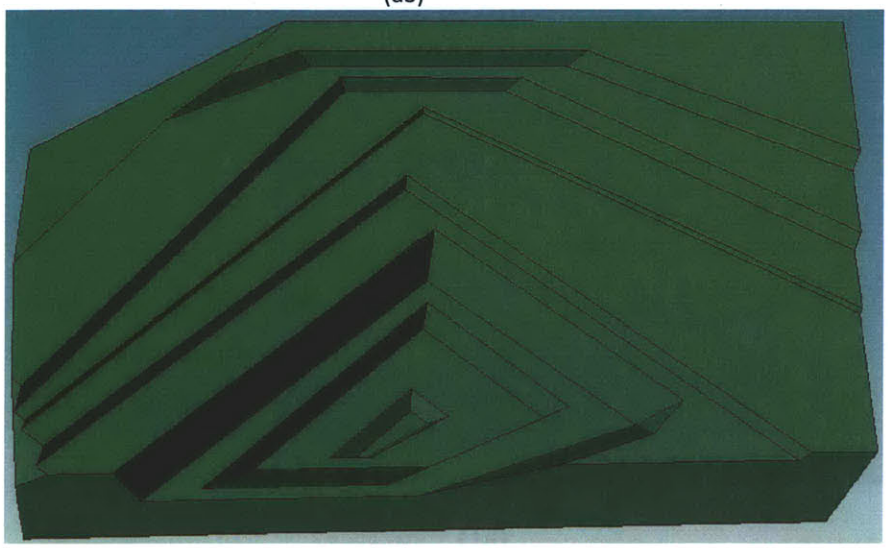

(b1)

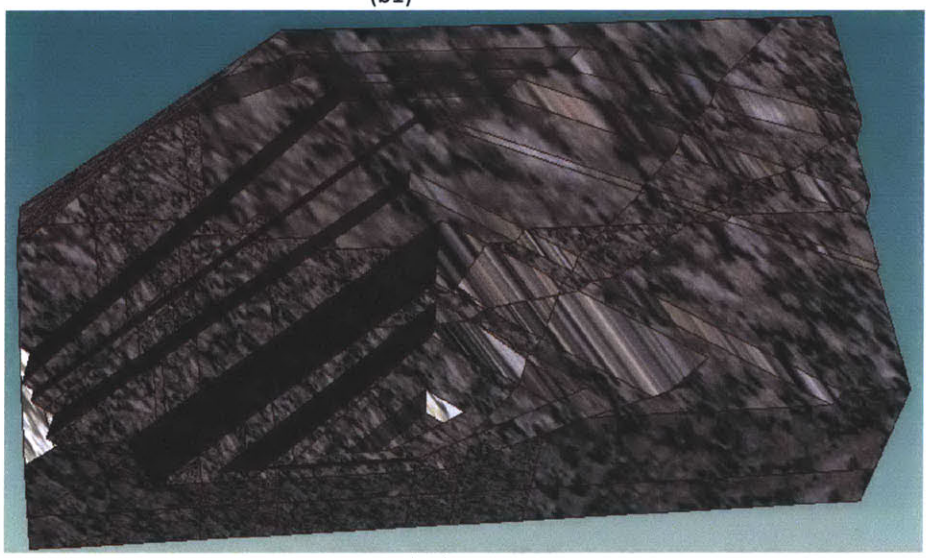

(b2)

Fig. 6-5 (a) Cutting a slope in a jointed rock mass (b) cutting a soil slope

The proposed 3D-NMM software also can be applied to various important engineering projects. Underground mining is one of them. Underground mining refers to various underground mining techniques used to excavate hard minerals, such as gold, copper, zinc, nickel and lead, but also involves using the same techniques for excavating ores of gems such as diamonds. Ground support is needed to secure the stability based on the stability analysis, and it can be further categorized into area support and local support. Apparently, the cost of conducting conventional analysis and support is extremely expensive. However, the proposed 3D-NMM software can

easily and precisely solve the problem, through the help of the function of 'support design'. Firstly, a numerical model of the underground mining is obtained through a couple steps of user's operations. Fig. 6-6 (a1) shows how the real underground mining structure looks like, and Fig. 6-6 (a2) shows the numerical 3-D model obtained by the proposed 3D-NMM software. Secondly, it is need to initialize the support design function. Fig. 6-6 (b) shows the how the function of 'support design' works and how it looks like. Finally, the analysis optimal results will be shown on the screen, which are based on the block theory.

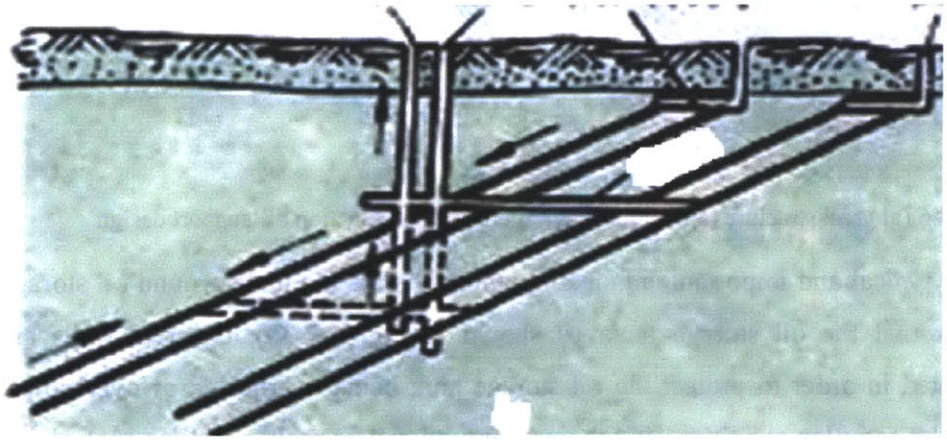

(a1) (Wikipedia)

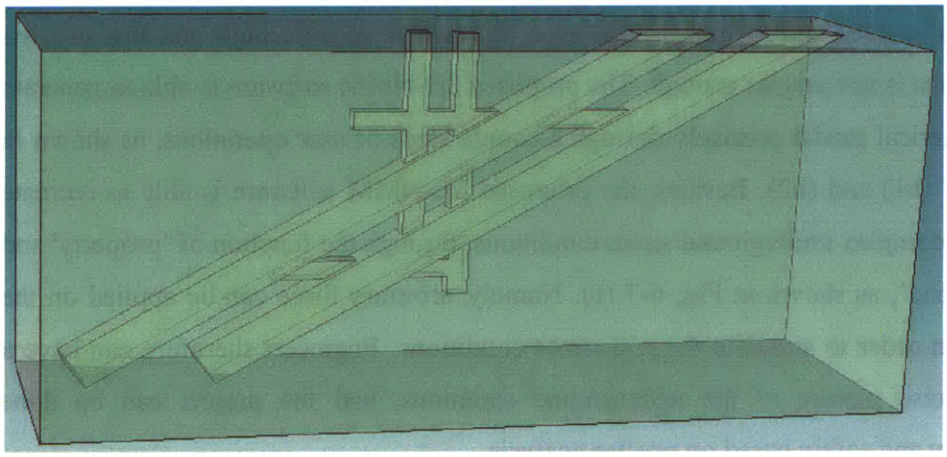

(a2)

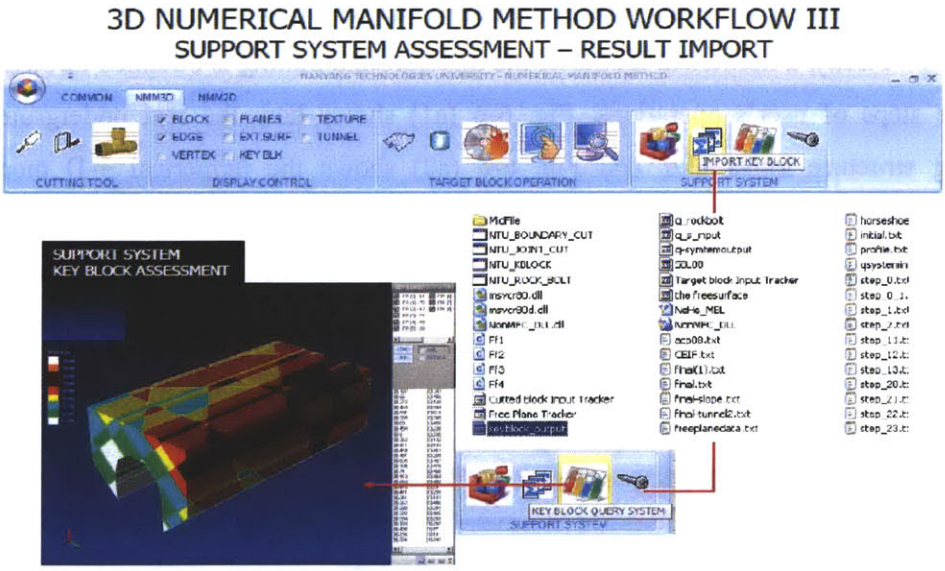

(b)

Fig. 6-6 (a1) real structure (a2) cutting shaft model (b) the function of 'support design'

Another typical and important engineering application is the underground oil storage tank. Around the oil storage tank, as shown in Fig. 6-7 (a), concrete walls are constructed in order to protect the oil storage tank being overheated or overcooled. Due to the complex conditions in the underground soil or rock, a precise analysis on the stress is essentially needed. For most of the cases, the analysis is based on the empirical curves and formulas. However, the cost is relative high and the analysis sometimes is not precise enough. The proposed 3D-NMM software is able to generate the numerical model precisely through a couple steps of user operations, as shown in Fig. 6-7 (b1) and (b2). Besides, the proposed 3D-NMM software is able to recreate the real complex underground stress conditions, through the function of 'property' and 'force load', as shown in Fig. 6-7 (c). Namely, arbitrary force can be applied on the planes in order to simulate the real stress conditions. Engineers therefore can have a full precise picture of the underground situations, and the project can be done smoothly and safely based on precise analysis.

(a) (Wikipedia)

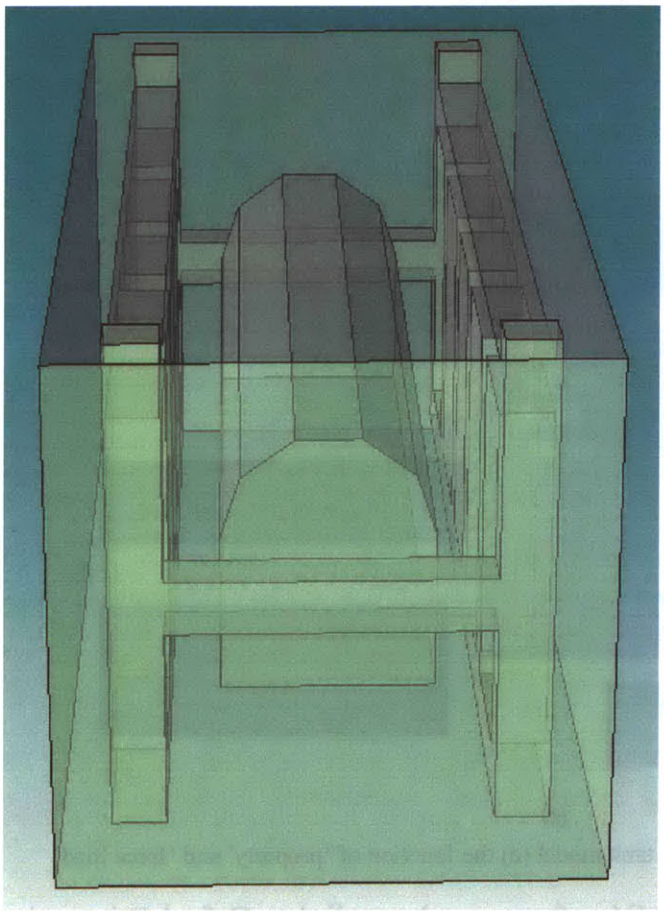

(b1)

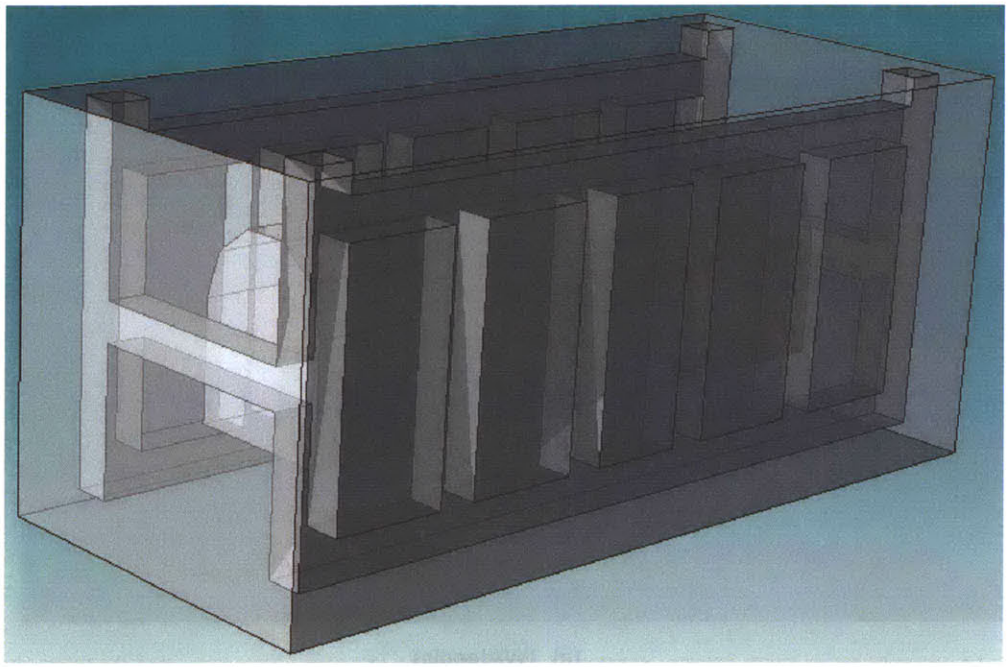

(b2)

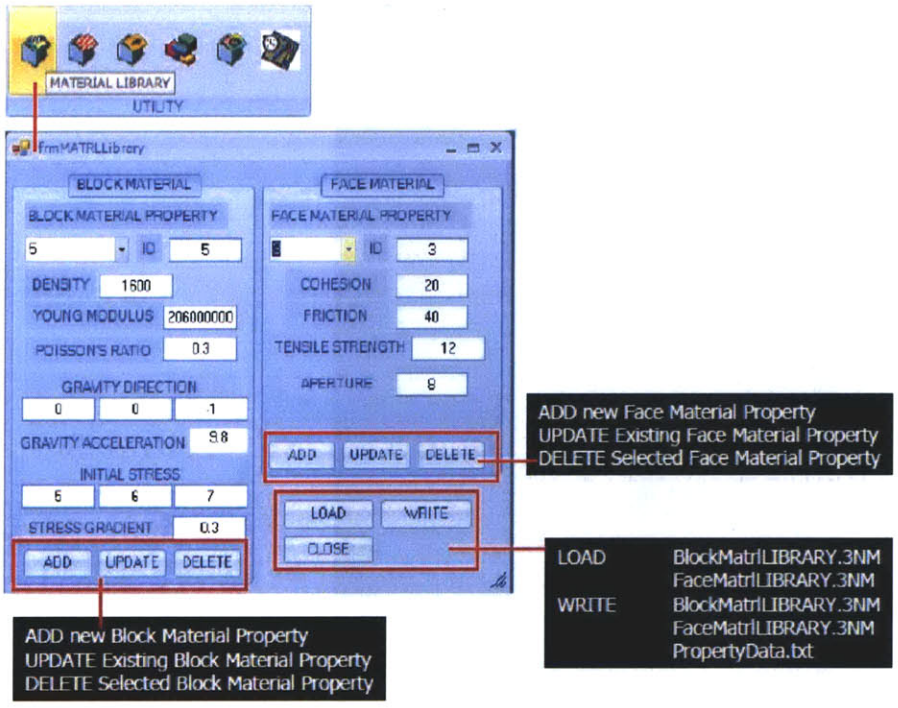

(c)

Fig. 6-7 (a) real structure (b) cutting tank model (c) the function of 'property' and 'force load'

Moreover, the proposed 3D-NMM software can be applied to Defend Science, i.e. some national security projects. Obviously, the national security matters are crucial to

any country. Some military weapons are stored inside specific underground caverns, and sometimes people can hide inside the underground caverns during the wars. Normally, stable passages are required to connect the underground cavern and the ground, and heavy transportations may be needed. Definitely, safety is the most important issue here. The underground cavern must withstand earthquake, bomb attack and so on. In order to get a precise analysis of the underground condition, again, it is needed the help of the proposed 3D-NMM software. As shown in Fig. 6-8, vivid numerical model is generated through the proposed 3D-NMM software. The stability and safety therefore can be guaranteed based on the precise analysis with the proposed 3D-NMM software.

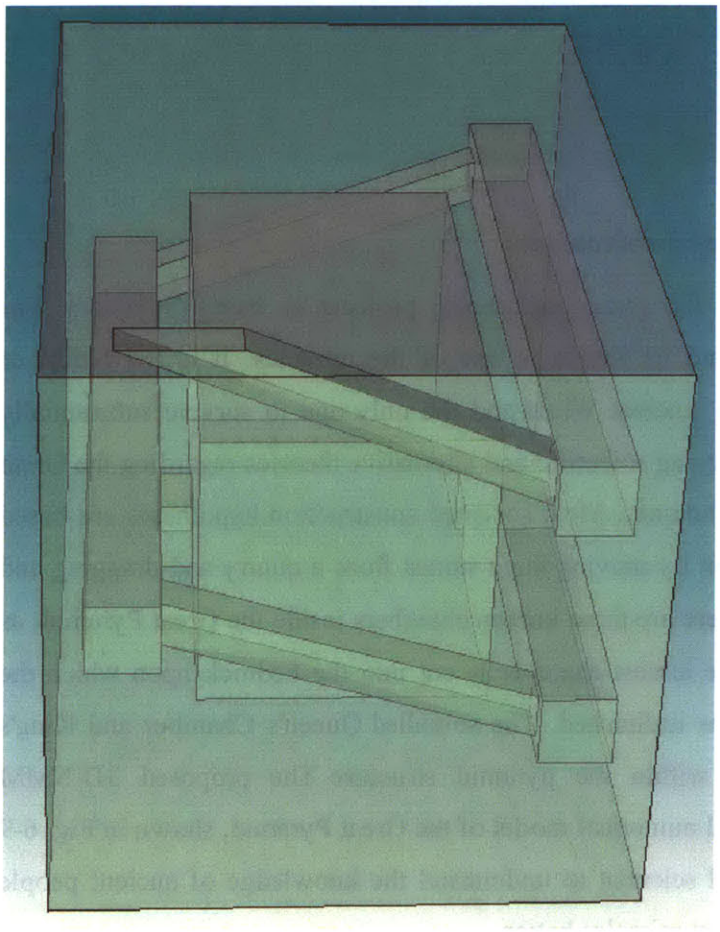

(a)

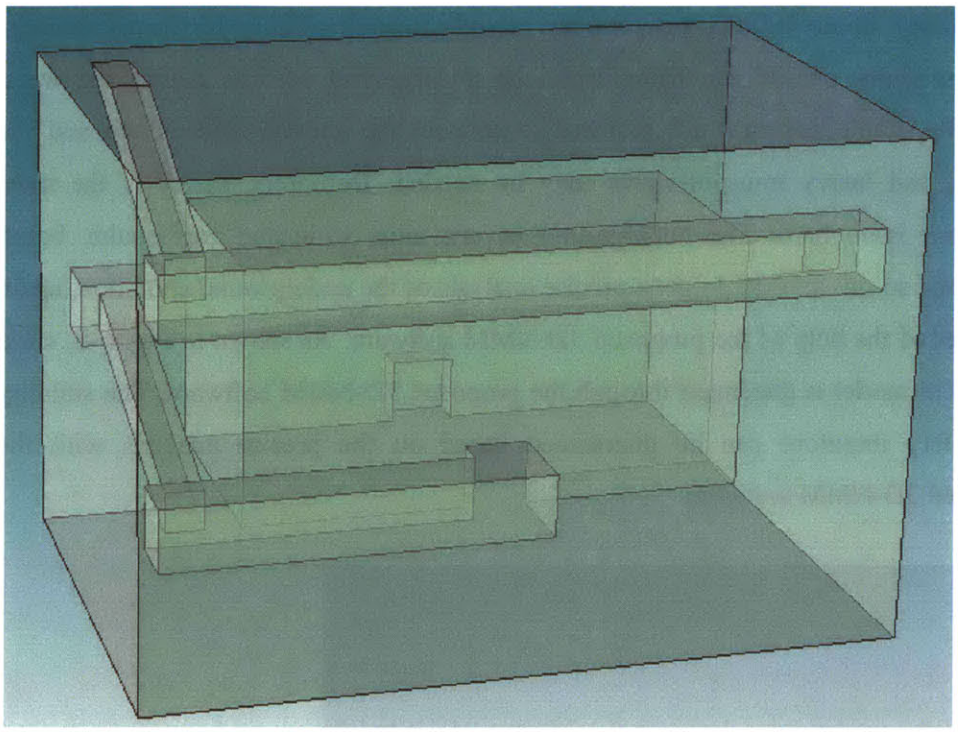

(b)

Fig. 6-8 cutting underground cavern with passages

The ancient miracles are the great engineering projects in human's history. For instance, the Great Pyramid of Khufu is one of the miracles. It is the oldest of the Seven Wonders of the Ancient World and the only one to survive substantially intact. There have been varying scientific and alternative theories regarding the Great Pyramid's construction techniques. Most accepted construction hypotheses are based on the idea that it was built by moving huge stones from a quarry and dragging and lifting them into place. There are three known chambers inside the Great Pyramid, as shown in Fig. 6-9 (a). The lowest chamber is cut into the bedrock upon which the pyramid was built and was unfinished. The so-called Queen's Chamber and King's Chamber are higher up within the pyramid structure. The proposed 3D-NMM software can generate vivid numerical model of the Great Pyramid, shown in Fig. 6-9 (b). It helps engineers and scientist to understand the knowledge of ancient people better and protect the ancient miracles better.

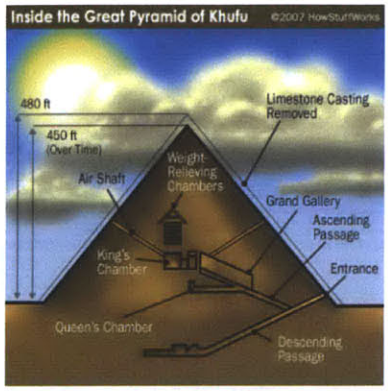

(a) (Wikipedia)

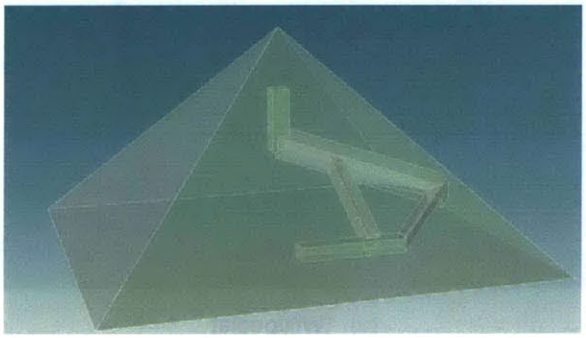

(b)

Fig. 6-9 cutting the Great Pyramid of Khufu: (a) real structure; (b) 3D cutting result

The Great Wall of China, one of the greatest wonders of the world, was listed as a World Heritage by UNESCO in 1987. As shown in Fig. 6-10 (a), just like a gigantic dragon, the Great Wall winds up and down across deserts, grasslands, mountains and plateaus, stretching approximately 8,851.8 kilometers (5,500 miles) from east to west of China. With a history of more than 2000 years, some of the sections are now in ruins or have disappeared. However, it is still one of the most appealing attractions all around the world owing to its architectural grandeur and historical significance. Again, with the help of the proposed 3D-NMM software, user can easily generate a numerical model of the Great Wall of China, as shown in Fig. 6-10 (b) and (c). With the convenient functions of the proposed 3D-NMM software, the external view and internal view can be clearly presented in front of user.

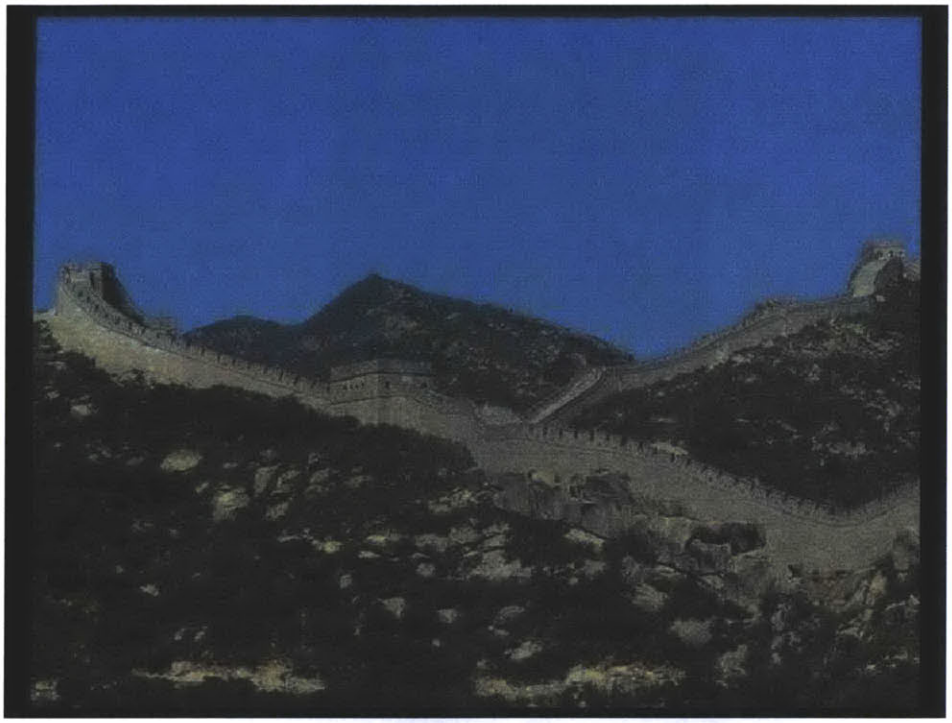

(a) (Wikipedia)

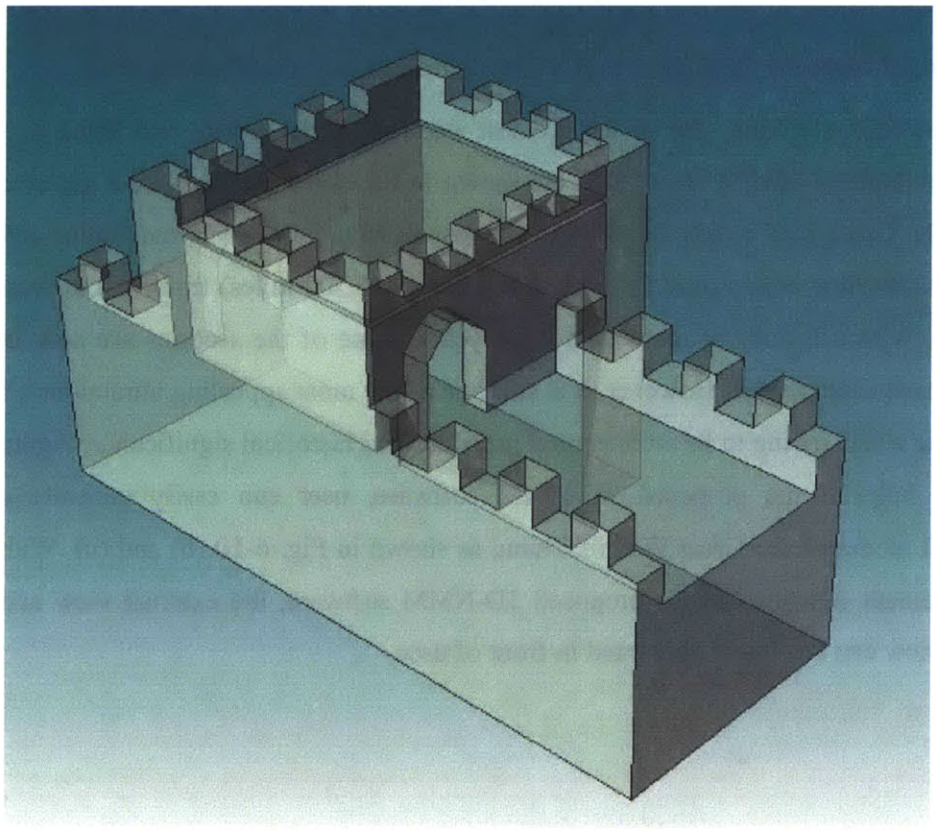

(b)

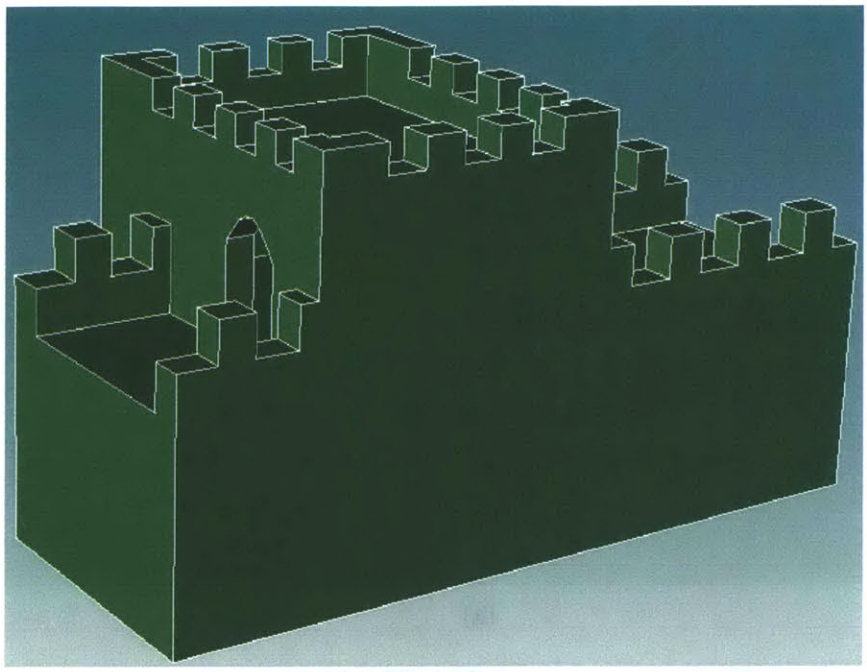

(c)

Fig. 6-10 cutting the Great Wall of China: (a) real structure; (b) 3D cutting result; (c) 3D cutting with external surfaces

Finally, some more examples are elaborated in order to further illustrate the convenience and the strength of functions of the proposed 3D-NMM software. In real situations, rocks normally have finite discontinuities within the body, namely some discontinuities are totally inside the body while some are connecting to the surface. However, most of the current softwares do not have this function, or some may make it by other means not precisely. On the other hand, the proposed 3D-NMM software includes this function through its own algorithm. As shown in Fig. 6-11 (a) and (b), two completed cutting 3-D numerical models, one with tunnel, are arbitrarily added in finite discontinuities. Some of the discontinuities are connecting to the surface, while some are totally inside or intersecting with the tunnel. Furthermore, that finite plane inside blocks is another important function of the proposed 3D-NMM software. For instance, in some rock stratums, finite planes exist inside the rock body. Normally, they are ignored or considered as negligible, due to the lack of approaches to handle with the extreme complex situations caused by these finite planes. However, this is not precise and sometimes may differ much with the real situation. As shown in Fig. 6-11 (c), this function is included within the proposed 3D-NMM software. Again, this illustrates the strength of the proposed 3D-NMM software.

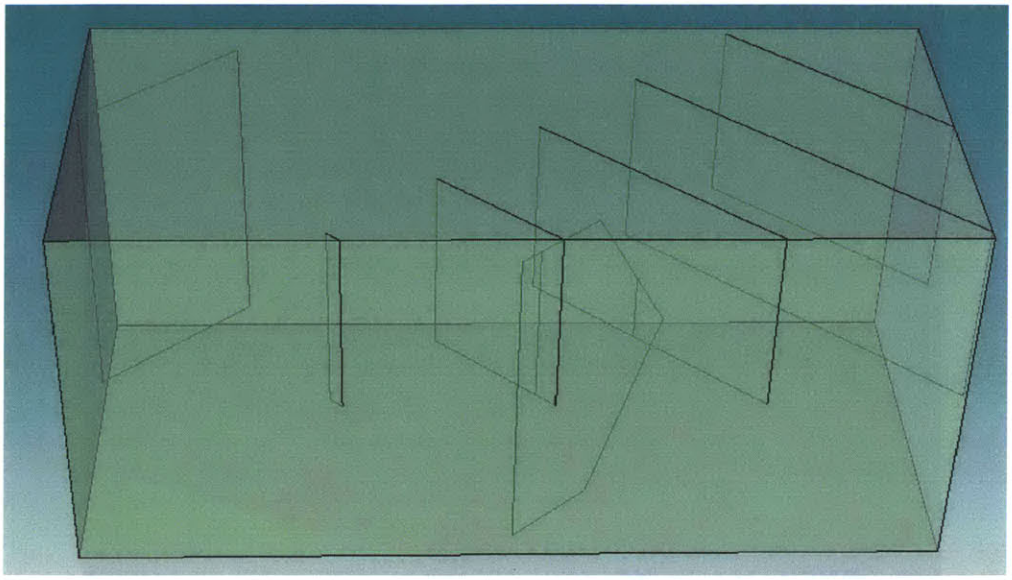

(a)

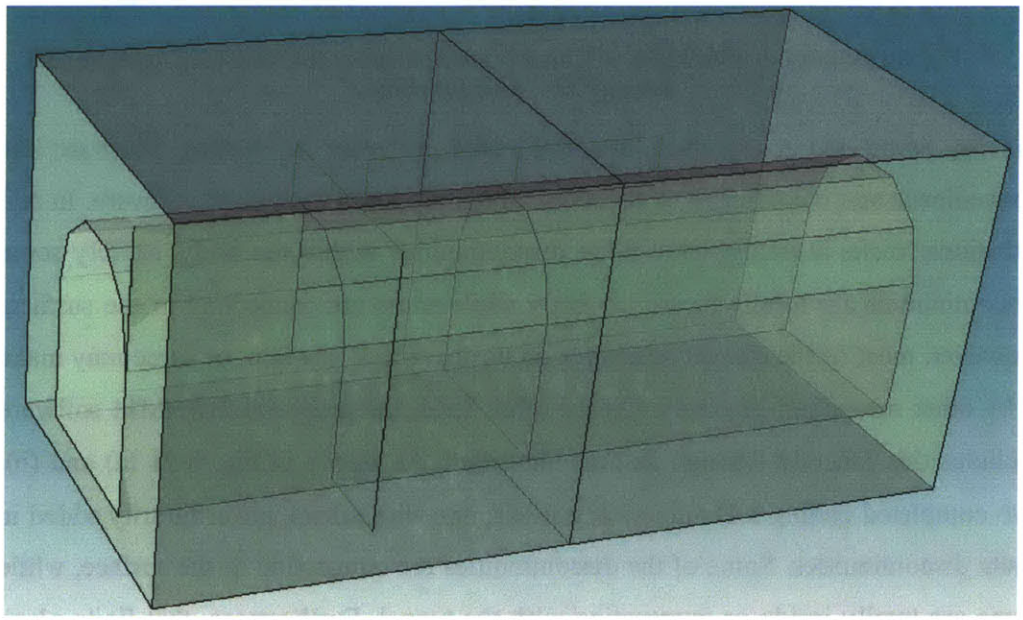

(b)

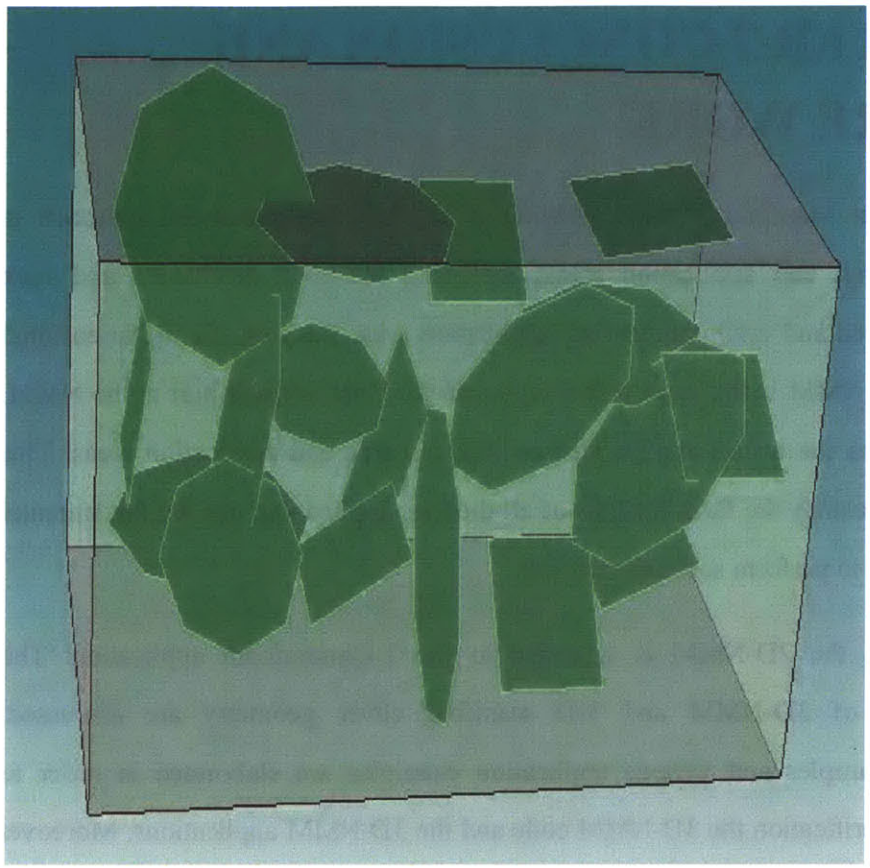

(c)

Fig. 6-11: (a) rectangular block model with arbitrary discontinuities; (b) tunnel model with arbitrary discontinuities; (c) cubic model with finite planes inside.

CHAPTER 7 CONCLUSION AND FUTURE WORK

The Numerical Manifold Method (NMM) is a promising numerical approach in various research and application areas, including the rock mechanics and rock engineering area and civil engineering application area. Besides, the 3-Dimensional version of the NMM is the latest technology and the most difficult part in the NMM. However, it has the widest applications in both research and application areas. This thesis aims to clarify the fundamentals of all theories applied and use the fundamental stage software to perform some simulations.

In this thesis, the 2D-NMM is extended to the 3-Dimensional application. The fundamentals of 3D-NMM and 3-D manifold cover geometry are discussed. Numerical examples and various application examples are elaborated in order to support and verification the 3D-NMM code and the 3D-NMM applications. Moreover, some simple examples are elaborated in order to illustrate the block cutting and the application of 3D-NMM in both continuous and discontinuous problems.

All these satisfied verification results of the 3D-MM program put a solid stage for its further development. In the next stage, the most suitable contact model to the 3-D NMM will be found.

In the near future, the proposed 3D-MM program will be widely accepted and applied in various industries with high accuracy, such as the mining industry in the western part of Australia. This numerical approach could be combined with the 'detecting sensors' and experimental results in some areas, for instance, cavern, tunnels, etc. Meanwhile, they can support and verify each other.

REFERENCES

[0] some pictures are from www.wikipedia.com

[1] Barton, N.R., Lien, R. and Lunde, J., Engineering classification of rock masses for the design of tunnel support. Rock Mech., 1974, 6, 189-239.

[2] Bieniawski Z. T. Rock Mechanics Design in Mining and Tunnelling. p272. Balkema, Rotterdam. 1984

[3] Bronstein, A.M. Bronstein, M.M. Kimmel, R. Weighted distance maps computation on parametric three-dimensional manifolds. Journal of Computational Physics, 2007.225: 771-784.

[4] Chappell, B.A.J, Deformational response in discontinuity, Rock Mech Min Sci and Geomech Abstr, 1979, 16(6):377-390

[5] Cheng, Y. M., Zhang, Y. H.: Coupling of FEM and DDA methods. Int. J. Geomech. 2002, 2(4), 503–517.

[6] Cheng, Y.M., and Zhang, Y.H., "Formulation of a three-dimensional numerical manifold method with tetrahedron and hexahedron elements", Rock Mechanics and Rock Engineering, 41,4, 2008, pp 601-628.

[7] Cundall, P.A.. A computer model for simulating progressive, large scale movements in blocky rock systems, Proceedings, International Symposium on Rock Fracture, Nancy, France, II-8, 1971.

[8] Desai, C.S., Zamman, M.M., Lightner, J.G., Siriwardane, H.J.. Thinlayer element for interfaces and joints. International Journal for Numerical and Analytical Methods in Geomechanics, 1984, 8:19-43.

[9] Ghaboussi, J., Wilson, E.L, Isenberg, J.. Finite element for rock joints and

interfaces. Journal of the Soil Mechanics and Foundations, ASCE, 1973, 99(10): 849-862.

[10] Goodman, R.E., Taylor, R.L., Brekke, T.L.. A model for the mechanics of jointed rock. Journal of the Soil Mechanics and Foundations Division, ASCE, 1968, 94: 637-659.

[11] Harrison JP, Hudson JA., Engineering on rock mechanics. Part 2: Illustrative workable examples. In: Sarkka P, Eloranta P, editors. Oxford: Pergamon. 2000

[12] Hoek, E. and Bray, J.W, Rock slope engineering, (2nd edition), London: The Institution of Mining and Metallurgy, 1977

[13] Itasca Conculting Group, Inc. (2003). 3 Dimensional Distinct Element Code-Theory and Background, Version 3.0. Minneapolis Press, Minnesota.

[14] Jiang, Q. H.: Research on three dimensional discontinuous deformation analysis method, PhD Dissertation. Wuhan Institute of Rock & Soil Mechanics. 2000

[15] Jiao, Y. Y.: Three dimensional DDA and Its Application. PhD Dissertation. Wuhan Institute of Rock & Soil Mechanics. 1998

[16] Jing L., A review of techniques, advances and outstanding issues in numerical modeling for rock mechanics and rock engineering, Int J Rock Mech Min Sci, 2003 40:283-353

[17] Katona, M.G.. A simple contact–friction interface element with applications to buried culverts. International Journal for Numerical and Analytical Methods in Geomechanics, 1983, 7: 371-384.

[18] Lang, T.A., Theory and practice of rock bolting. Trans. Am. Inst. Min. Engrs., 1991, 220, 333-348.

[19] Li, S.C. Li, S.C. Cheng, Y.M. (2005). Enriched meshless manifold method for

two-dimensional crack modeling. Theoretical and Applied Fracture Mechanics, 44: 234-248.

[20] Long J.C.S, Remer J.S., Wilson C.R and Witherspoon P.A., Porous media equivalents for networks of discontinuous fractures, Water Resour Res, 1982 18(3):645-58

[21] Ma, G.W., An, X.M., He, L. The numerical manifold method-A reivew. Submitted to International Journal of Computational Methods, 2009.

[22] Mauldon M, Goodman RE. Vector analysis of keyblock rotation. J Geotech Geoenviron Eng (ASCE). 1996;122(12):976-87.

[23] Moes, N., Dolbow, J., Belytschko, T.. A finite element method for crack growth without remeshing. International Journal for Numerical Methods in Engineering, 1999, 46: 131-150.

[24] Munjiza, A.. The combined finite-discrete element method, Wiley, Chichester, 2004.

[25] N.Barton, R.Lien and J.Lunde. "Engineering Classification of Rock Masses for the Design of Tunnel Support". Norwegian Geotechnical Insitute. NR.106. 1974

[26] Nooshin, H, Disney, P and Champion, O. Computer Aided Processing of Polyhedric Configurations. Beyond the Cube: The Architecture of Space Frames and Polyhedra, 1997. chapter 12: 343-384.

[27] Richard E. Goodman and Shi Genhua. Block Theory and its Application to Rock Engineering. 1985. p295-330.

[28] S.Chen, Y.-N.Oh, D.-S.Jeng and L.-k.Chien, Analysis of displacement and stress around a tunnel, Stability of Rock Structures, Hatzor 2002

[29] Shi, G.H.. Discontinuous Deformation Analysis – A new numerical model for the

static and dynamics of block systems, PhD Dissertation, Department of Civil Engineering, U.C. Berkeley, 1988.

[30] Shi, G.H.. Manifold method of material analysis, Trans. 9th Army Conf. on Applied Mathematics and Computing, Minneapolis, Minnesota, 1991, pp.57-76.

[31] Shi, G.H. Producing Joint Polygons, cutting joint blocks and finding key blocks for general free surfaces. Chinese Journal of Rock Mechanics and Engineering, 2006. 25: 2161-2170.

[32] Strouboulis, T., Babuska, I., Copps, K.. The design and analysis of the generalized finite element method, Computer Methods in Applied Mechanics and Engineering, 2000, 181: 43-69.

[33] Sukumar, N., Prevost, J.H.. Modeling quasi-static crack growth with the extended finite element method Part I: computer implementation. International Journal of Solids and Structures, 2003, 40: 7513-7537.

[34] Terada, K. Asai, M. Yamagishi, M.. Finite cover method for linear and non-linear analyses of heterogeneous solid. International Journal for Numerical Method in Engineering, 2003. 58:1321-1346.

[35] Tonon F. Generation of Mauldon's and Goodman's analysis of keyblock rotations. J Geotech Geoenviron Eng (ASCE). 1998;124(10):913-22.

[36] Wang, R. L., Chen, N. M., Liu, B. S.: Theory analysis of 3D-DDA. Chin. J. Rock Mech.Engng. 1996,15, 219–224.

[37] Windsor, C.R., Rock Reinforcement System, Int. J. Rock Mech. Min. Sci. 1997, Vol. 43, No 6, pp. 919-951

[38] Zienkiewicz, O.C., Best, B., Dullage, C., Stagg, K.. Analysis of nonlinear problems in rock mechanics with particular reference to jointed rock systems.

Proceedings of the Second International Congress on Rock Mechanics, Belgrade, 1970, pp. 8-14.